

Accretion and Outflows in MRI Turbulent Proto-planetary Disks.



Mario Flock
Natalia Dzyurkevich
Hubert Klahr
Neal Turner
Thomas Henning

MFU III - Zakopane 21 – 27. August

Overview

I. Turbulent viscosity profile

II. Accretion Flows

III. From Outflows to Disk wind

IV. Dynamo

Overview

I. Turbulent viscosity profile

II. Accretion Flows

III. From Outflows to Disk wind

IV. Dynamo



Flock et al. 2010
Flock et al. 2011

Disk model based
on Fromang & Nelson 2006



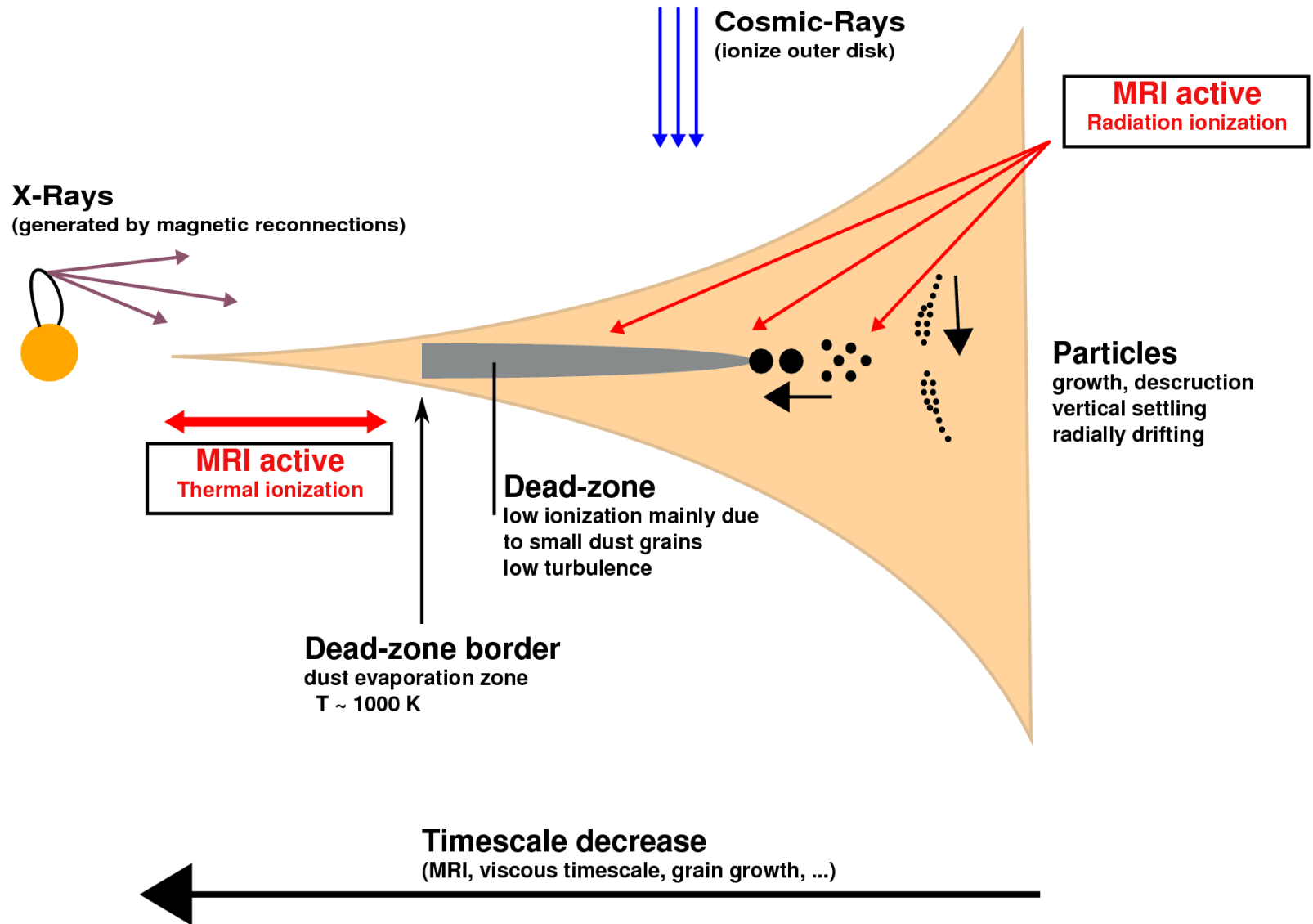
ApJ sub.

MRI activity in Proto-planetary disk

Magneto Rotational Instability (MRI)

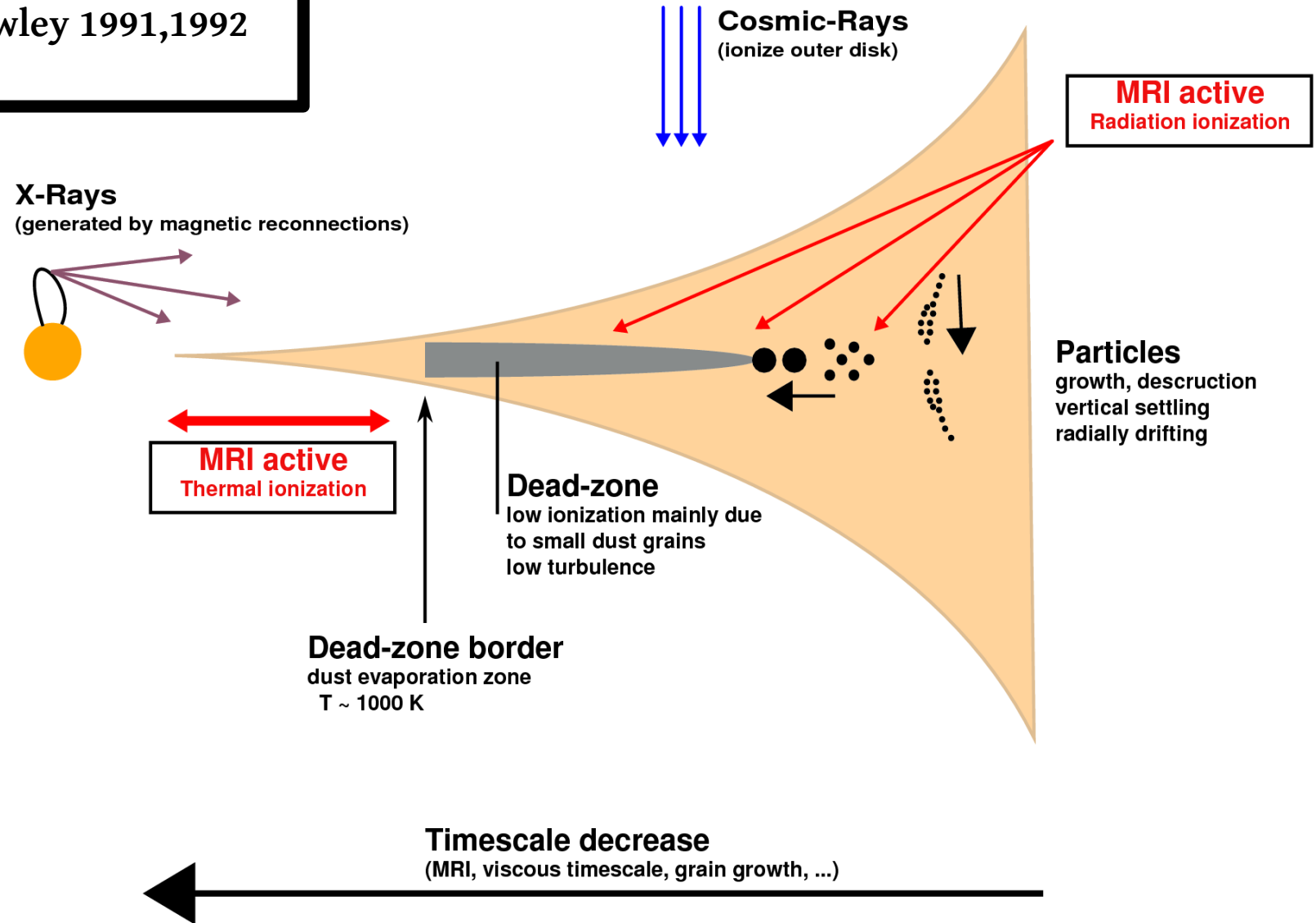
- weak magnetic fields
- shear
- good ionization

MRI activity in Proto-planetary disk

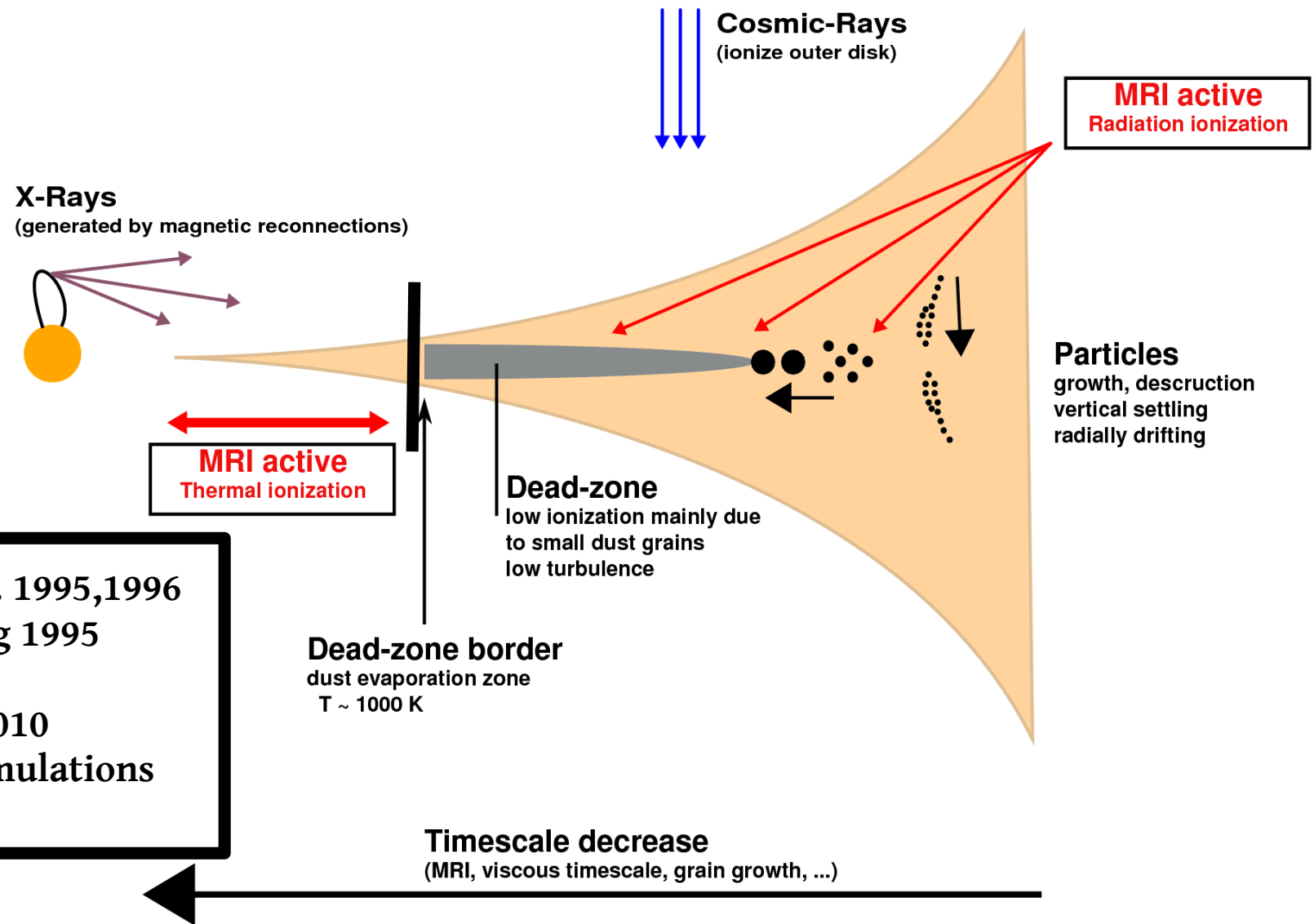


MRI activity in Proto-planetary disk

Balbus & Hawley 1991,1992

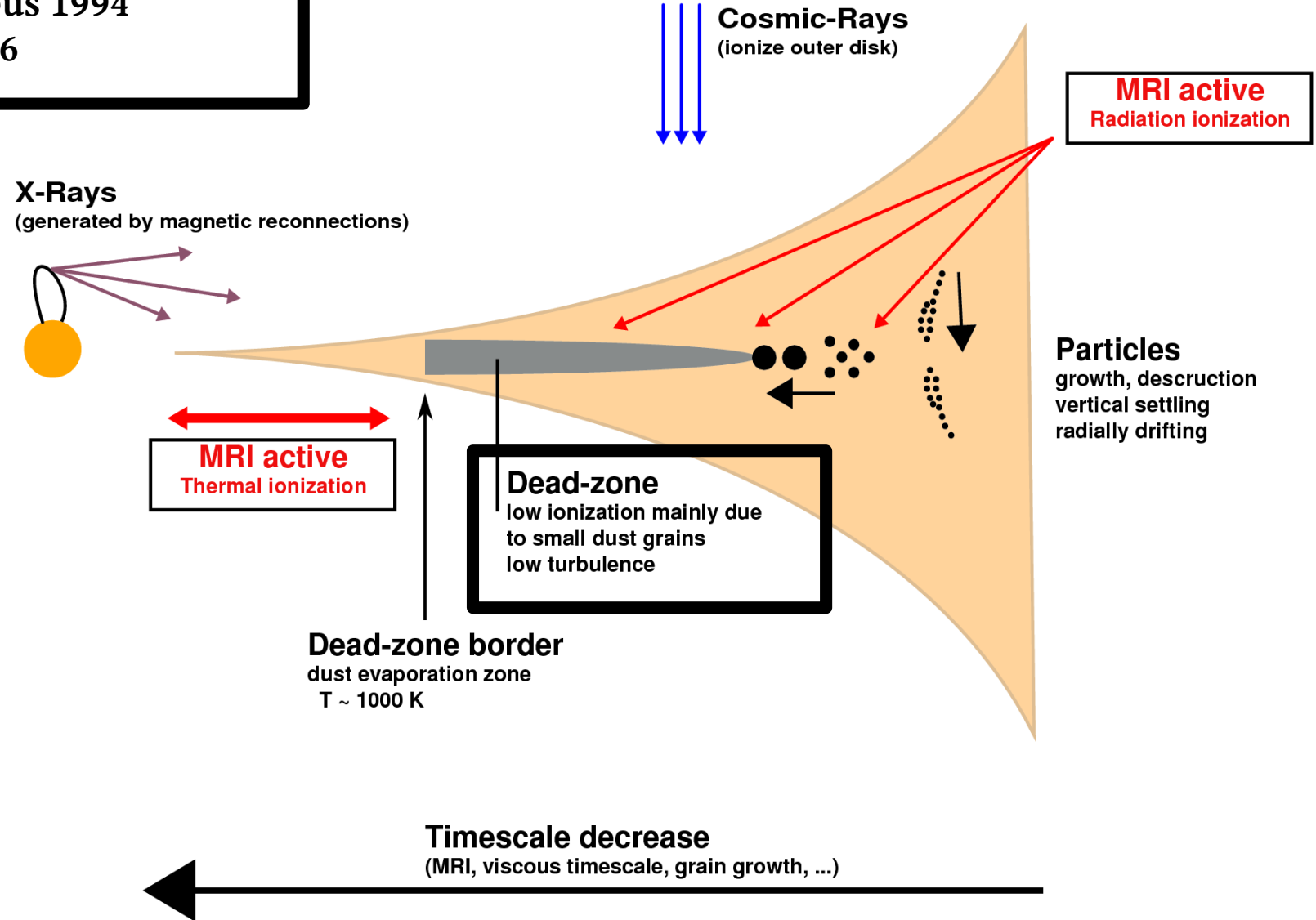


MRI activity in Proto-planetary disk

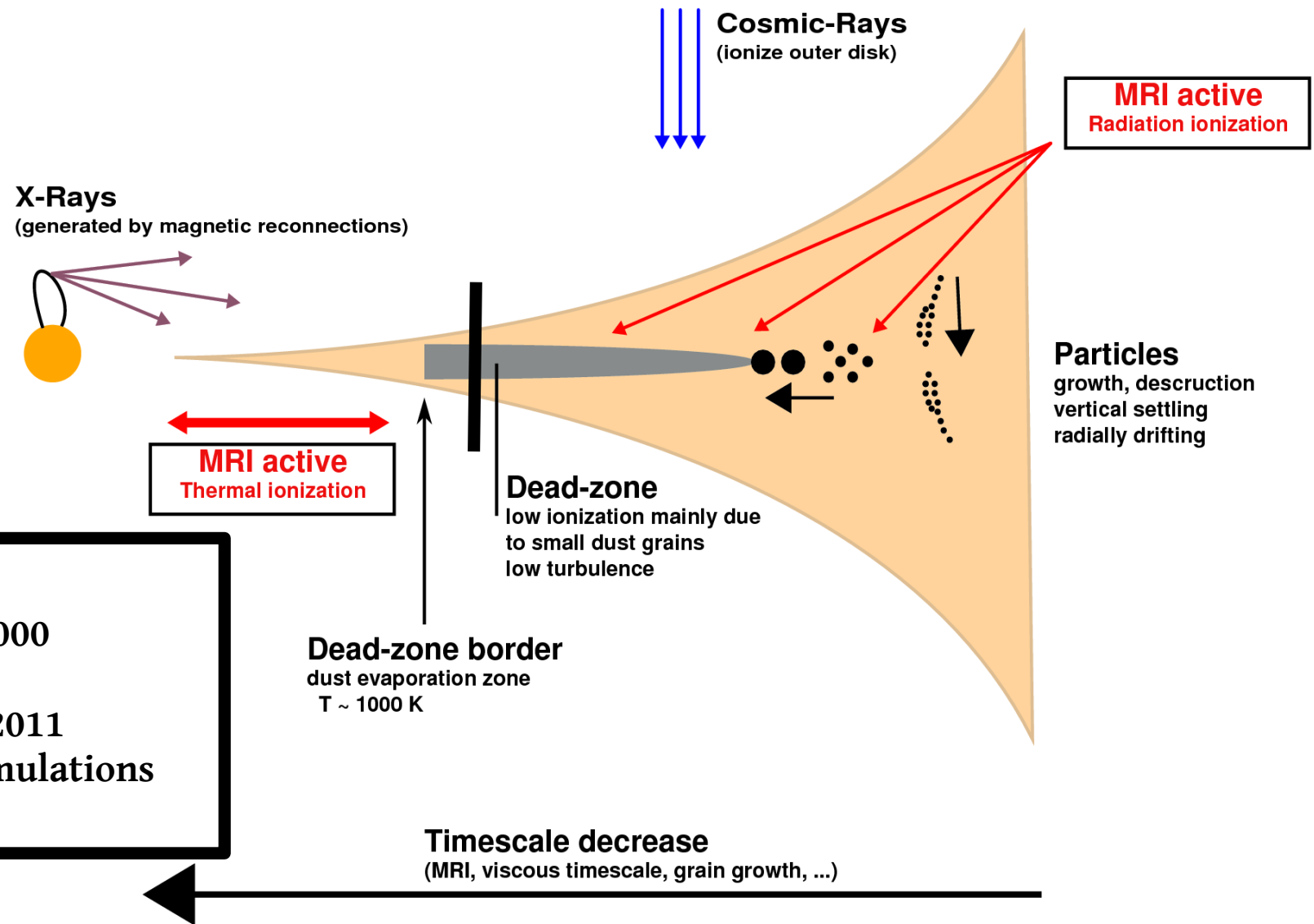


MRI activity in Proto-planetary disk

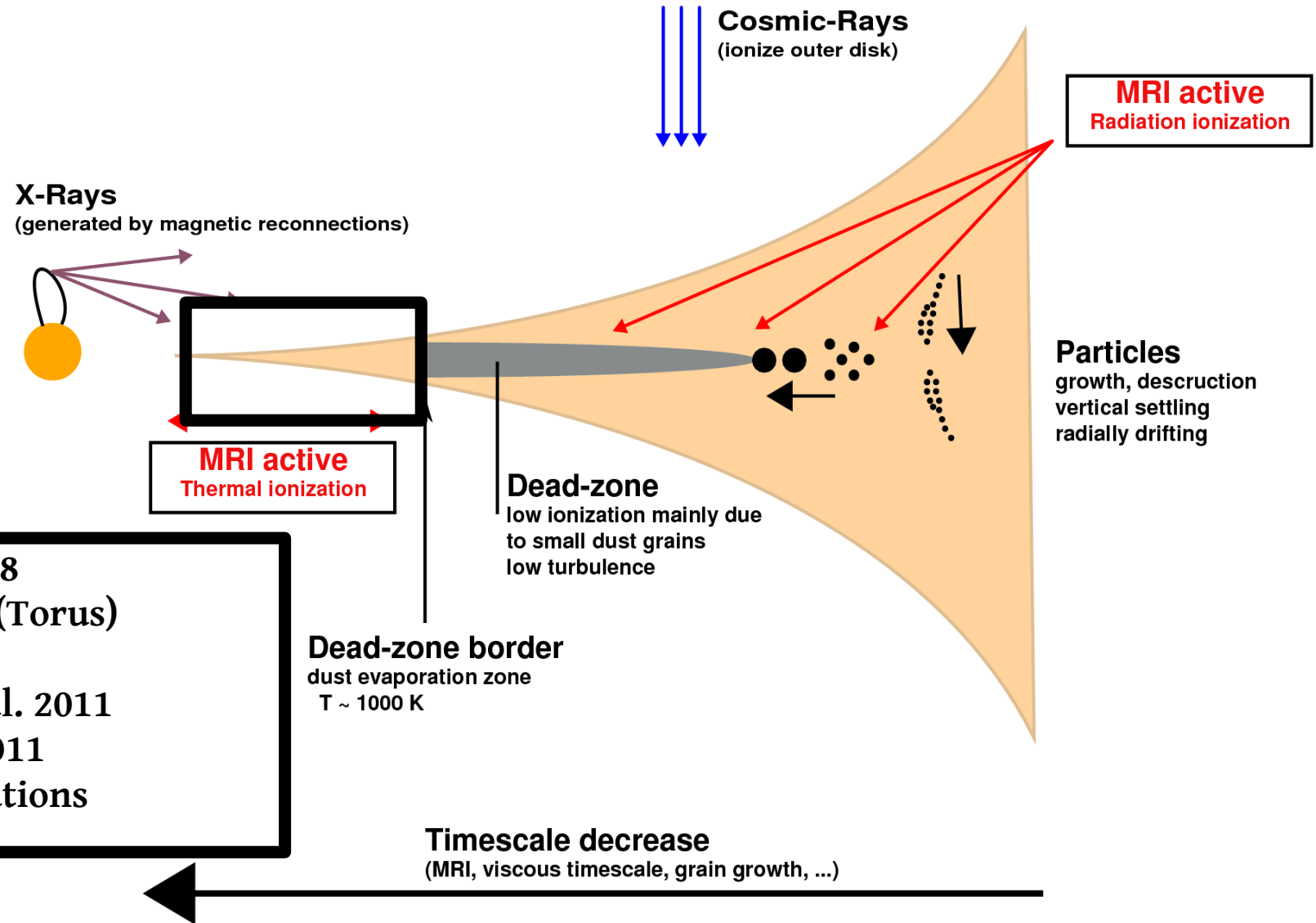
Blaes & Balbus 1994
Gammie 1996



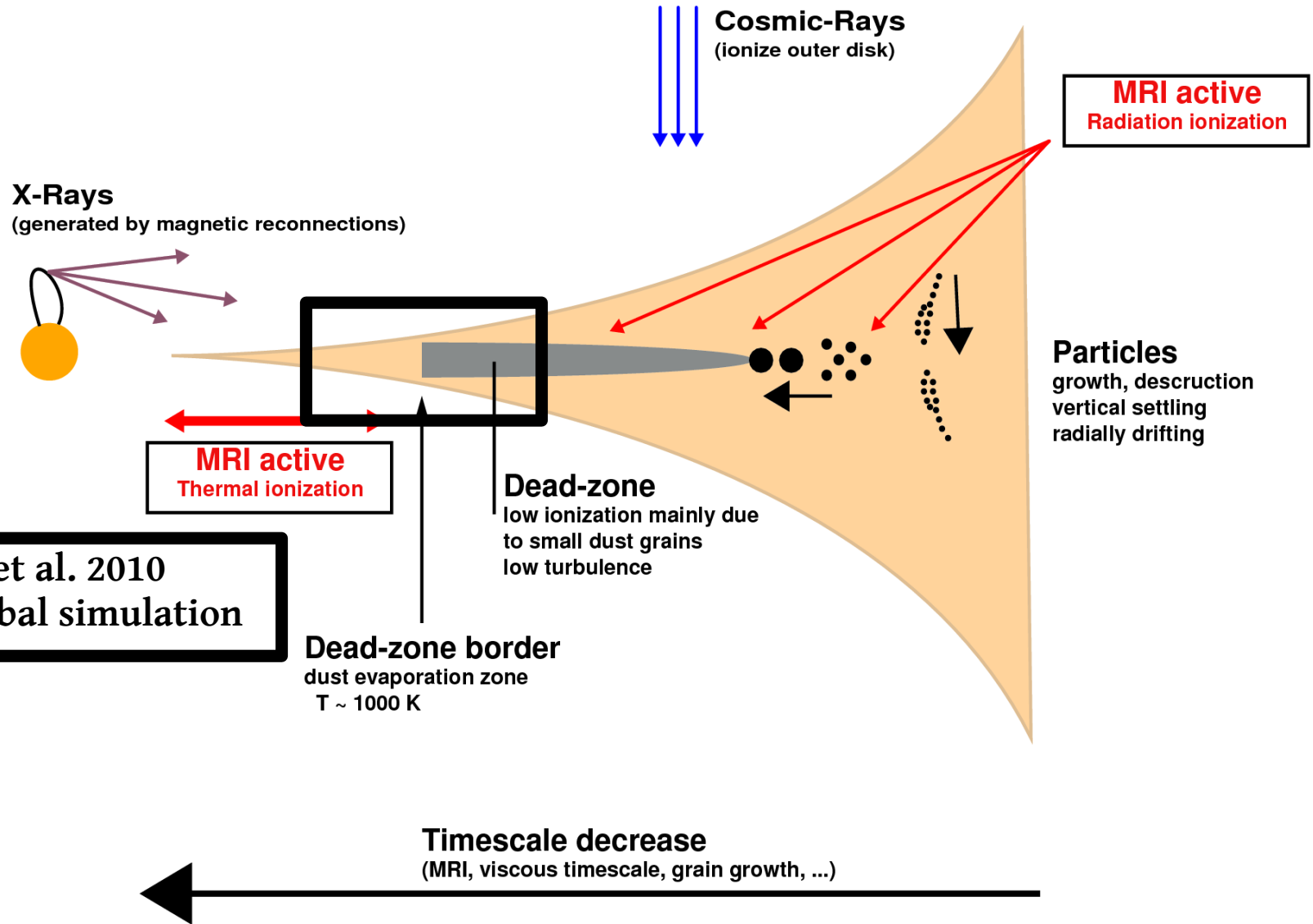
MRI activity in Proto-planetary disk



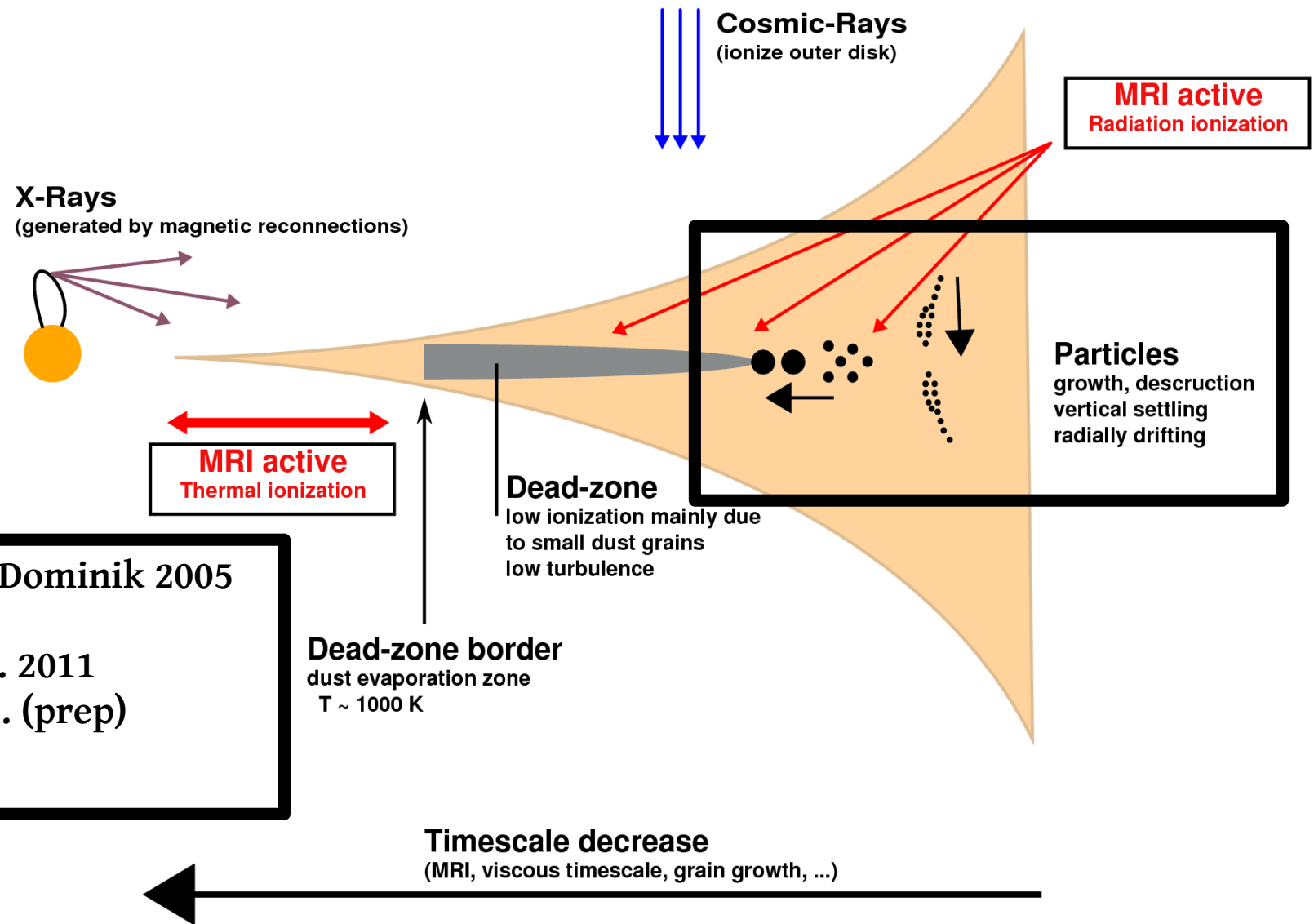
MRI activity in Proto-planetary disk



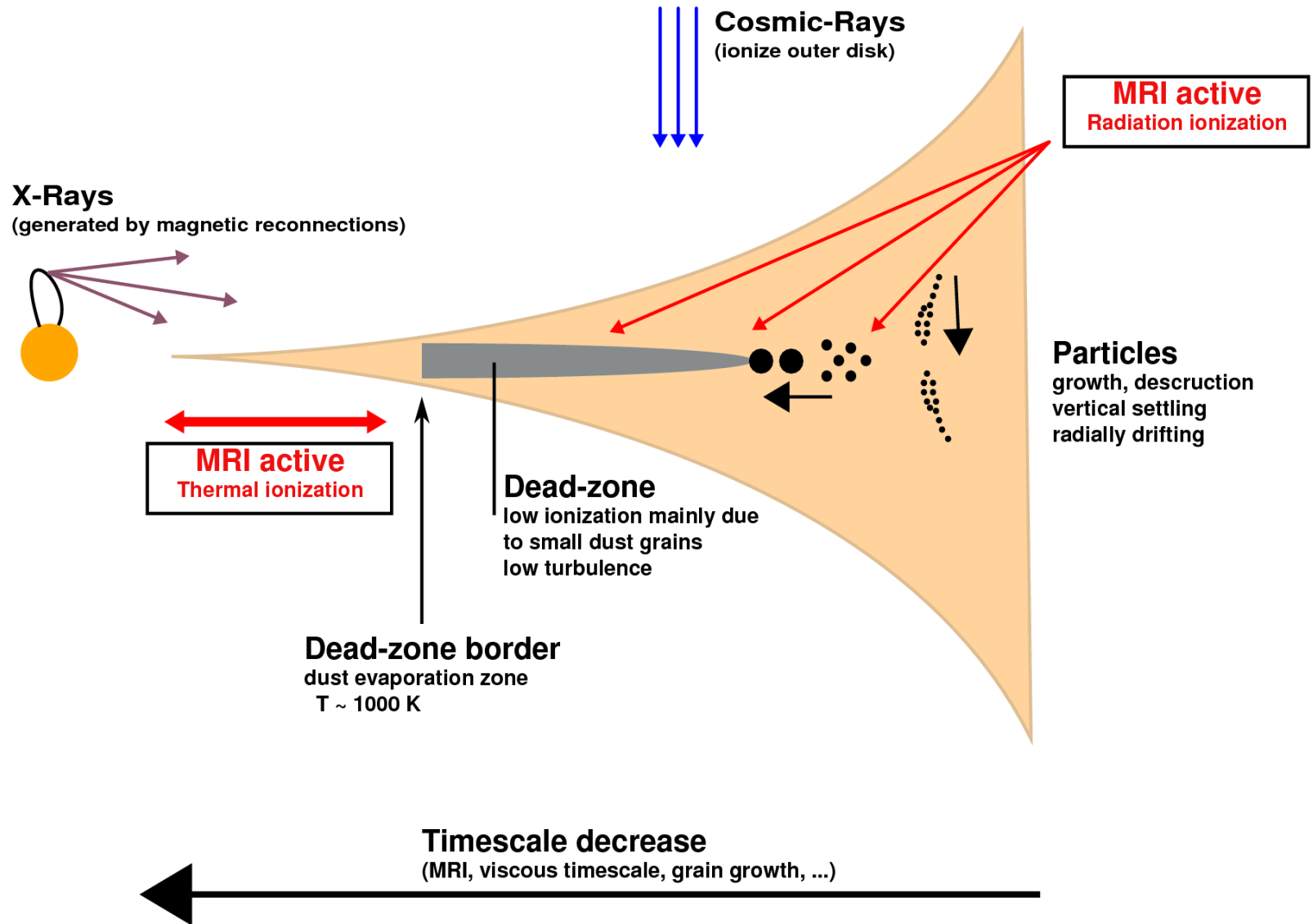
MRI activity in Proto-planetary disk



MRI activity in Proto-planetary disk



MRI activity in Proto-planetary disk



TURBULENCE AND STEADY FLOWS IN THREE-DIMENSIONAL GLOBAL STRATIFIED MAGNETOHYDRODYNAMIC SIMULATIONS OF ACCRETION DISKS

M. FLOCK¹, N. DZYURKEVICH¹, H. KLAHR¹, N. J. TURNER^{1,2}, AND TH. HENNING¹

¹ Max Planck Institute for Astronomy, Königstuhl 17, 69117 Heidelberg, Germany

² Jet Propulsion Laboratory, California Institute of Technology, Pasadena, CA 91109, USA

Received 2011 February 4; accepted 2011 April 21; published 2011 ???

ABSTRACT

We present full 2π global three-dimensional stratified magnetohydrodynamic (MHD) simulations of accretion disks. We interpret our results in the context of protoplanetary disks. We investigate the turbulence driven by the magnetorotational instability (MRI) using the PLUTO Godunov code in spherical coordinates with the accurate and robust HLLD Riemann solver. We follow the turbulence for more than 1500 orbits at the innermost radius of the domain to measure the overall strength of turbulent motions and the detailed accretion flow pattern. We find that regions within two scale heights of the midplane have a turbulent Mach number of about 0.1 and a magnetic pressure two to three orders of magnitude less than the gas pressure, while in those outside three scale heights the magnetic pressure equals or exceeds the gas pressure and the turbulence is transonic, leading to large density fluctuations. The strongest large-scale density disturbances are spiral density waves, and the strongest of these waves has $m = 5$. No clear meridional circulation appears in the calculations because fluctuating radial pressure gradients lead to changes in the orbital frequency, comparable in importance to the stress gradients that drive the meridional flows in viscous models. The net mass flow rate is well reproduced by a viscous model using the mean stress distribution taken from the MHD calculation. The strength of the mean turbulent magnetic field is inversely proportional to the radius, so the fields are approximately force-free on the largest scales. Consequently, the accretion stress falls off as the inverse square of the radius.

Key words: accretion, accretion disks – magnetic fields – magnetic reconnection – magnetohydrodynamics (MHD) – protoplanetary disks

Online-only material: animations

- 3D Full 2π stratified MHD simulation
- Over 1500 inner orbits
- Godunov code

TURBULENCE AND STEADY FLOWS IN THREE-DIMENSIONAL GLOBAL STRATIFIED MAGNETOHYDRODYNAMIC SIMULATIONS OF ACCRETION DISKS

M. FLOCK¹, N. DZYURKEVICH¹, H. KLAHR¹, N. J. TURNER^{1,2}, AND TH. HENNING¹

¹ Max Planck Institute for Astronomy, Königstuhl 17, 69117 Heidelberg, Germany

² Jet Propulsion Laboratory, California Institute of Technology, Pasadena, CA 91109, USA

Received 2011 February 4; accepted 2011 April 21; published 2011 ???

ABSTRACT

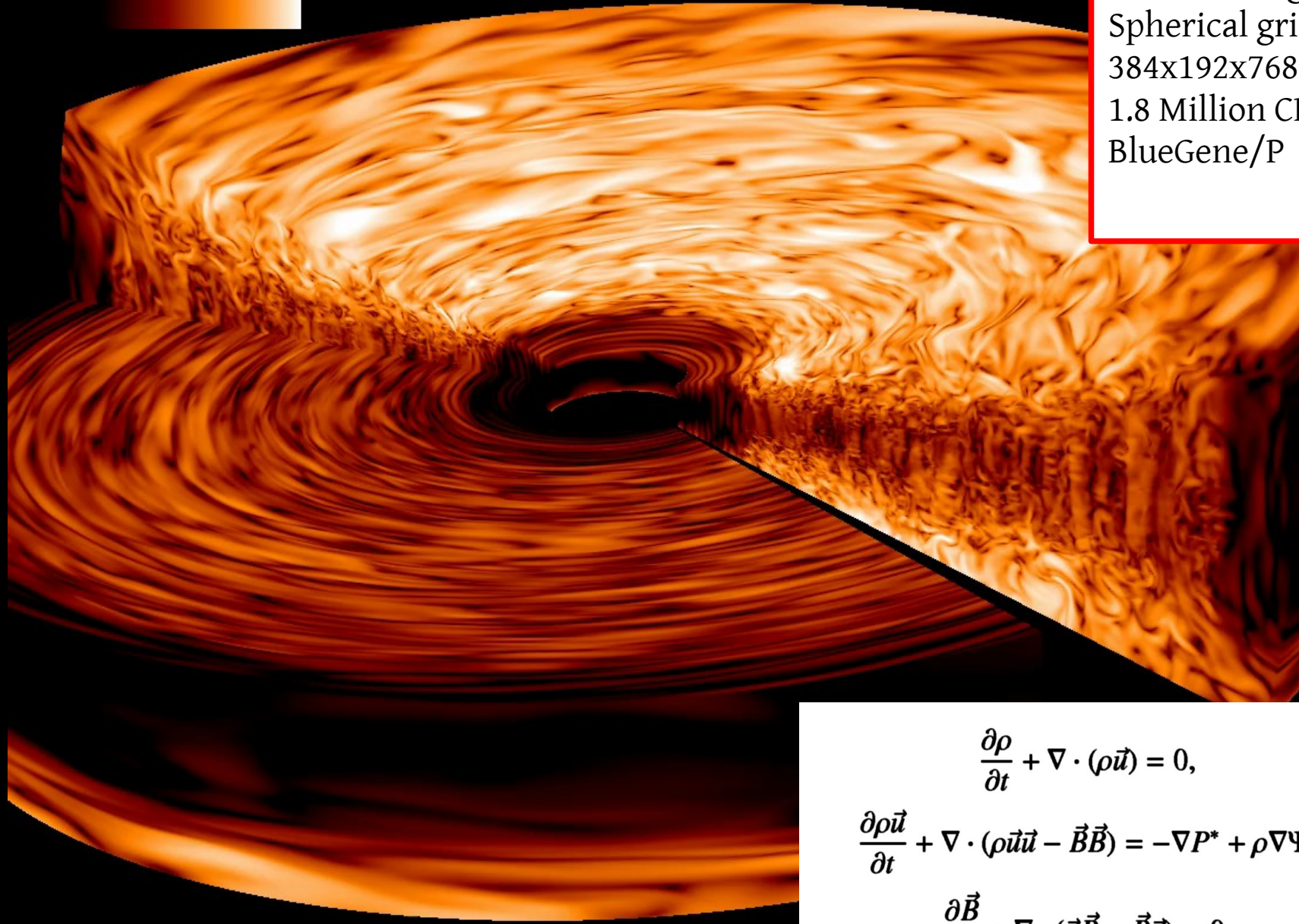
We present full 2π global three-dimensional stratified magnetohydrodynamic (MHD) simulations of accretion disks. We interpret our results in the context of protoplanetary disks. We investigate the turbulence driven by the magnetorotational instability (MRI) using the PLUTO Godunov code in spherical coordinates with the accurate and robust HLLD Riemann solver. We follow the turbulence for more than 1500 orbits at the innermost radius of the domain to measure the overall strength of turbulent motions and the detailed accretion flow pattern. We find that regions within two scale heights of the midplane have a turbulent Mach number of about 0.1 and a magnetic pressure two to three orders of magnitude less than the gas pressure, while in those outside three scale heights the magnetic pressure equals or exceeds the gas pressure and the turbulence is transonic, leading to large density fluctuations. The strongest large-scale density disturbances are spiral density waves, and the strongest of these waves has $m = 5$. No clear meridional circulation appears in the calculations because fluctuating radial pressure gradients lead to changes in the orbital frequency, comparable in importance to the stress gradients that drive the meridional flows in viscous models. The net mass flow rate is well reproduced by a viscous model using the mean stress distribution taken from the MHD calculation. The strength of the mean turbulent magnetic field is inversely proportional to the radius, so the fields are approximately force-free on the largest scales. Consequently, the accretion stress falls off as the inverse square of the radius.

Key words: accretion, accretion disks – magnetic fields – magnetic reconnection – magnetohydrodynamics (MHD) – protoplanetary disks

Online-only material: animations

Method
PLUTO code
2. order, HLLD
Flock et al 2010
Beckwith et al 2011

- 3D Full 2π stratified MHD simulation
- Over 1500 inner orbits
- Godunov code

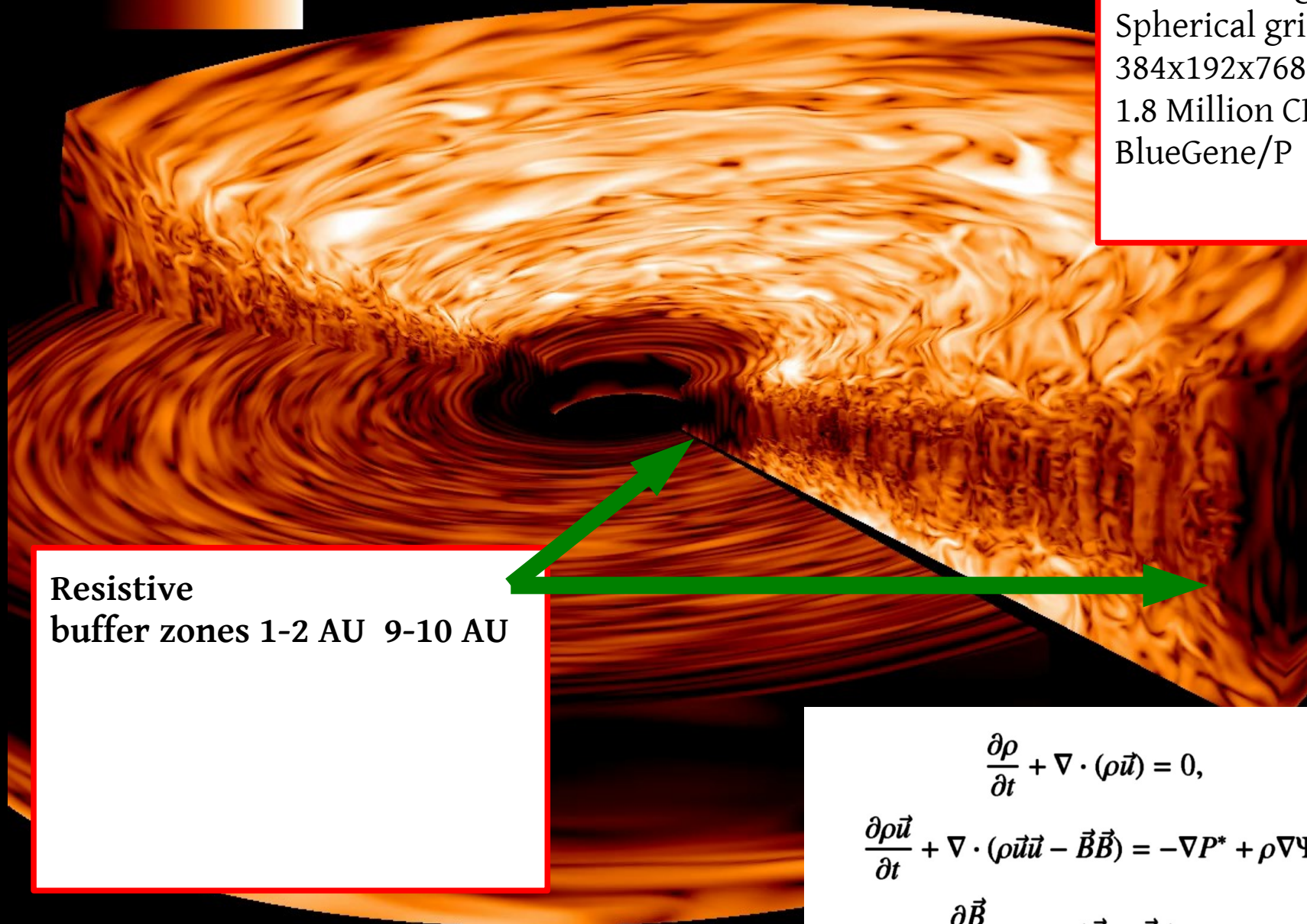


1-10 AU
8.6 scale heights
Spherical grid
384x192x768
1.8 Million CPU H
BlueGene/P

$$\frac{\partial \rho}{\partial t} + \nabla \cdot (\rho \vec{u}) = 0,$$

$$\frac{\partial \rho \vec{u}}{\partial t} + \nabla \cdot (\rho \vec{u} \vec{u} - \vec{B} \vec{B}) = -\nabla P^* + \rho \nabla \Psi,$$

$$\frac{\partial \vec{B}}{\partial t} + \nabla \cdot (\vec{u} \vec{B} - \vec{B} \vec{u}) = 0,$$

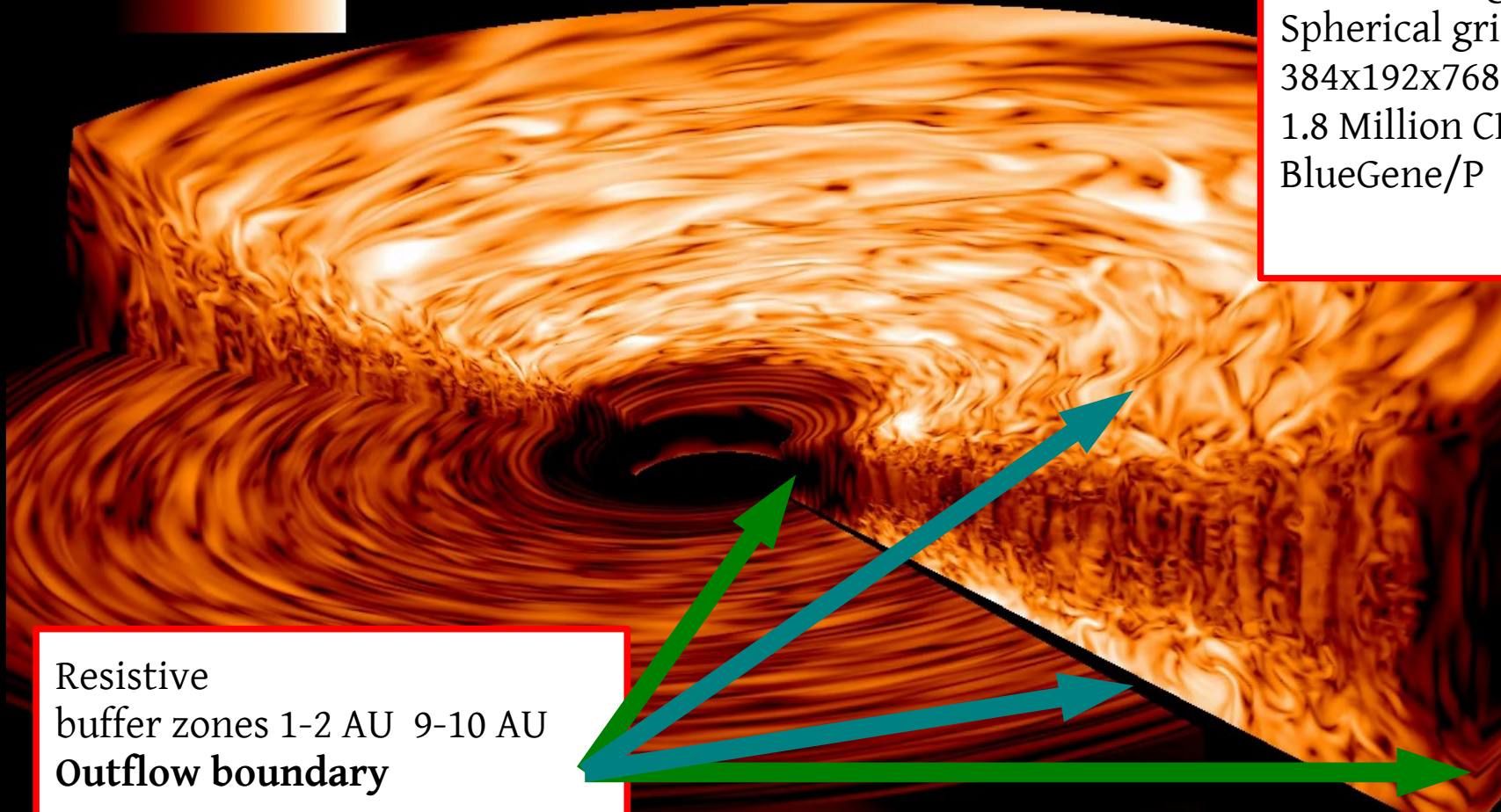


1-10 AU
8.6 scale heights
Spherical grid
384x192x768
1.8 Million CPU H
BlueGene/P

$$\frac{\partial \rho}{\partial t} + \nabla \cdot (\rho \vec{u}) = 0,$$

$$\frac{\partial \rho \vec{u}}{\partial t} + \nabla \cdot (\rho \vec{u} \vec{u} - \vec{B} \vec{B}) = -\nabla P^* + \rho \nabla \Psi,$$

$$\frac{\partial \vec{B}}{\partial t} + \nabla \cdot (\vec{u} \vec{B} - \vec{B} \vec{u}) = 0,$$

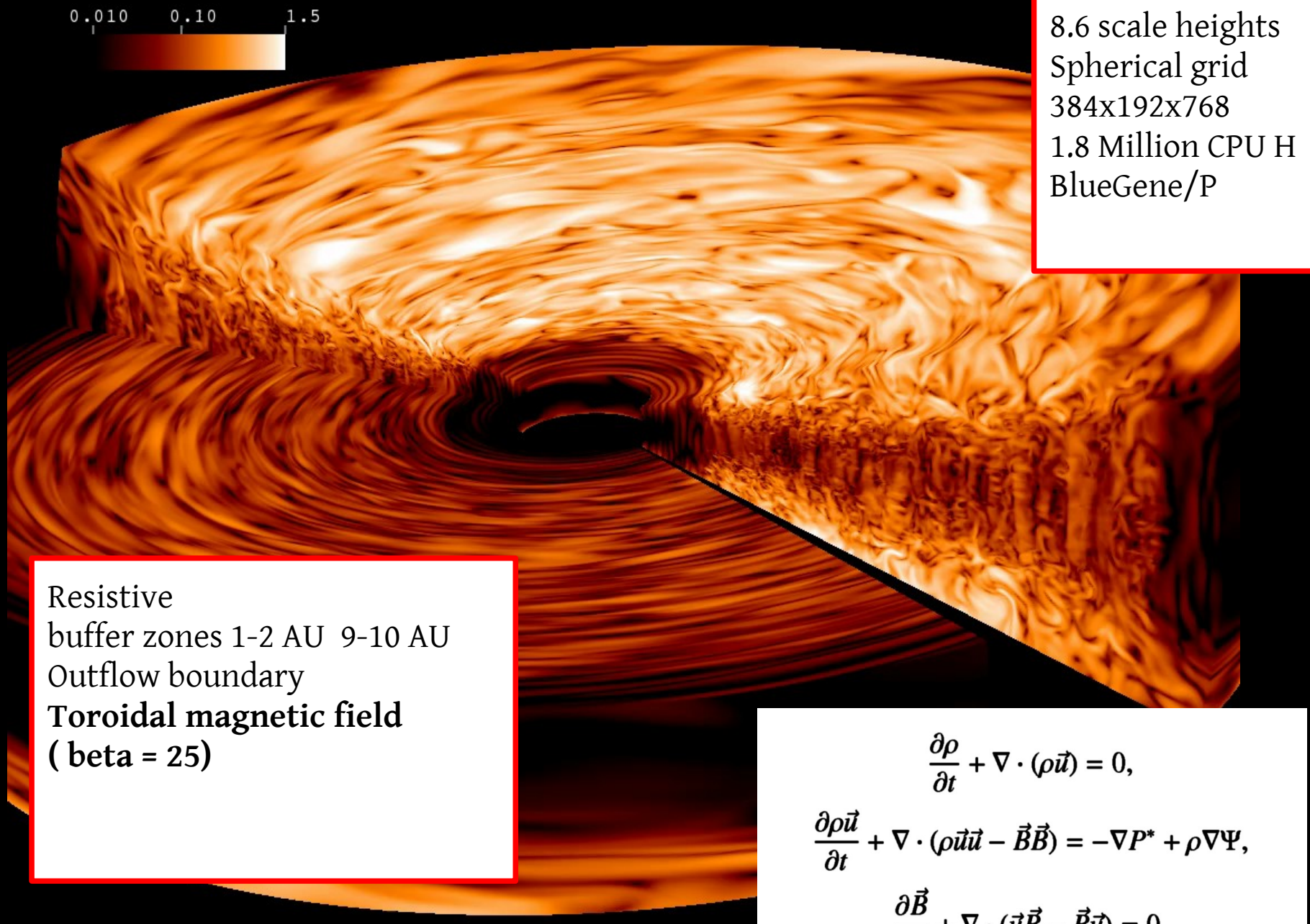


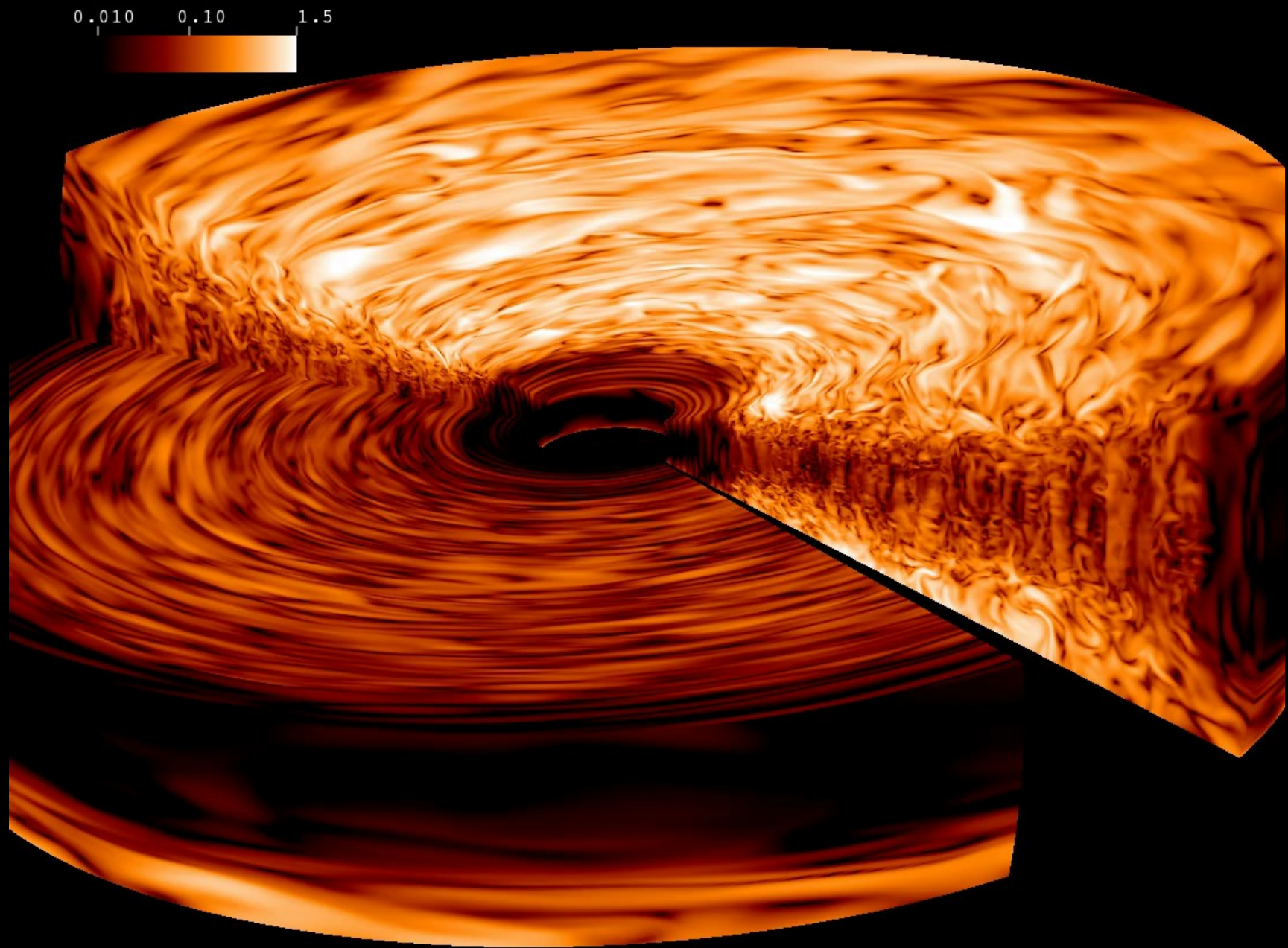
1-10 AU
8.6 scale heights
Spherical grid
384x192x768
1.8 Million CPU H
BlueGene/P

$$\frac{\partial \rho}{\partial t} + \nabla \cdot (\rho \vec{u}) = 0,$$

$$\frac{\partial \rho \vec{u}}{\partial t} + \nabla \cdot (\rho \vec{u} \vec{u} - \vec{B} \vec{B}) = -\nabla P^* + \rho \nabla \Psi,$$

$$\frac{\partial \vec{B}}{\partial t} + \nabla \cdot (\vec{u} \vec{B} - \vec{B} \vec{u}) = 0,$$





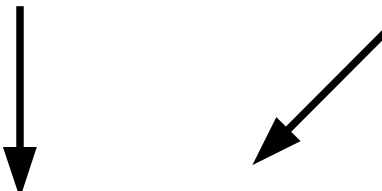
I. Turbulent viscosity profile

Important for disk evolution

- Surface density profile $\Sigma(r)$
 - Mass accretion rate
 - Input for dust coagulation models
- Summarized in the
Shakura-Sunyaev α -value

I. α profile

Reynolds Stress Maxwell Stress

$$\alpha = \frac{\int \rho \left(\frac{v'_\phi v'_R}{c_s^2} - \frac{B'_\phi B'_R}{4\pi\rho c_s^2} \right) dV}{\int \rho dV}$$


I. α profile

- Vertical profile
- Radial profile

$$\alpha = \frac{\int \rho \left(\frac{v'_\phi v'_R}{c_s^2} - \frac{B'_\phi B'_R}{4\pi\rho c_s^2} \right) dV}{\int \rho dV}$$

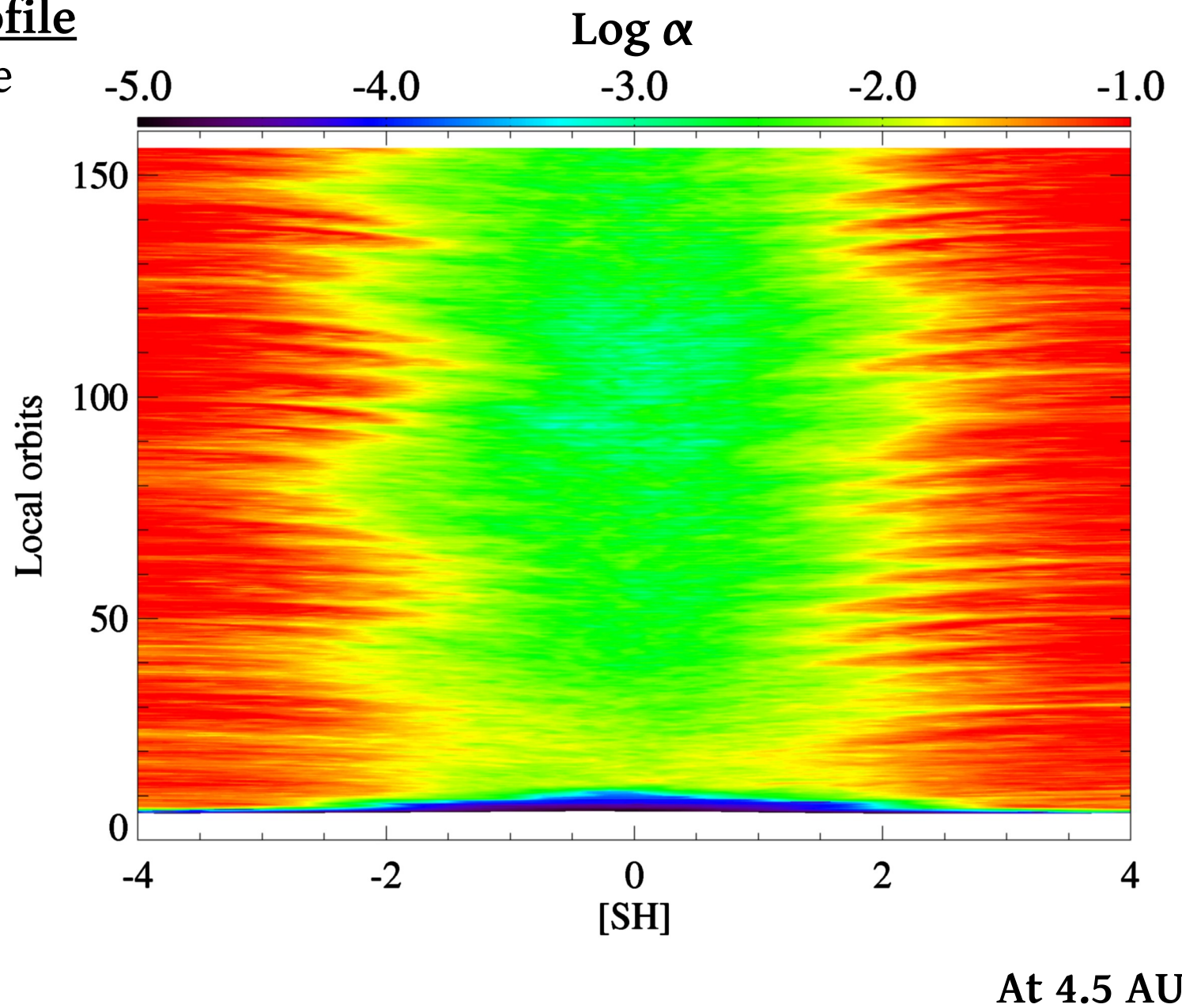
Reynolds Stress Maxwell Stress

The diagram illustrates the components of the Reynolds Stress term. A vertical arrow points to the term $\frac{v'_\phi v'_R}{c_s^2}$, and a diagonal arrow points to the term $\frac{B'_\phi B'_R}{4\pi\rho c_s^2}$.

At 4.5 AU

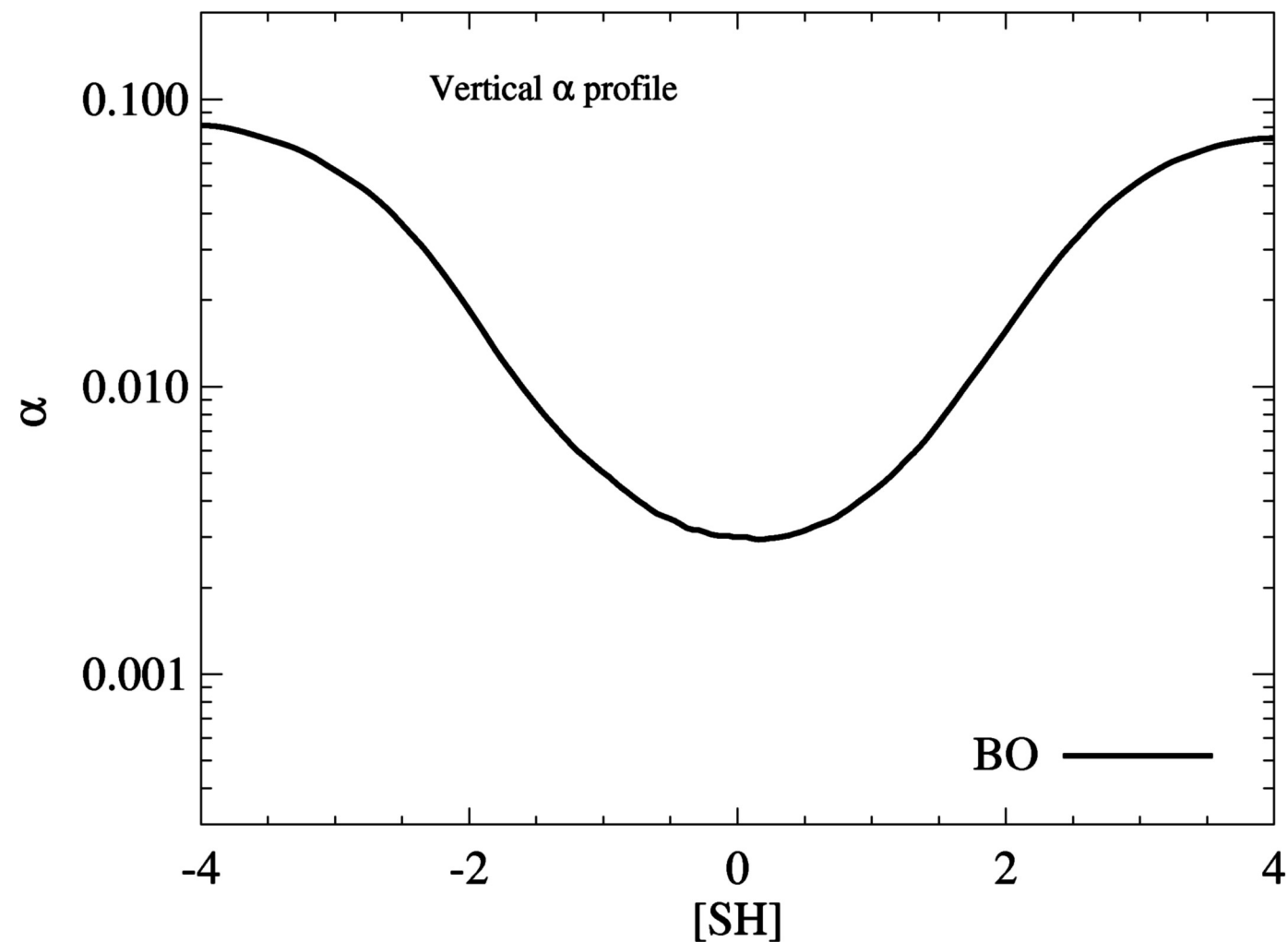
I. α profile

- Vertical profile
- Radial profile



I. α profile

- Vertical profile
- Radial profile

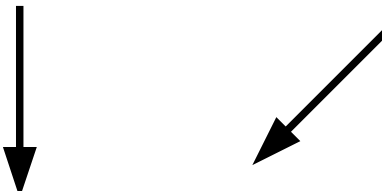


At 4.5 AU

I. α profile

- Vertical profile
- Radial profile

Reynolds Stress Maxwell Stress

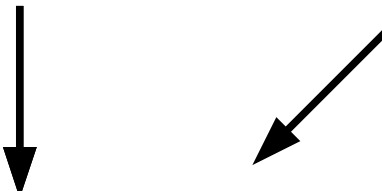
$$\alpha = \frac{\int \rho \left(\frac{v'_\phi v'_R}{c_s^2} - \frac{B'_\phi B'_R}{4\pi\rho c_s^2} \right) dV}{\int \rho dV}$$


I. α profile

- Vertical profile
- Radial profile

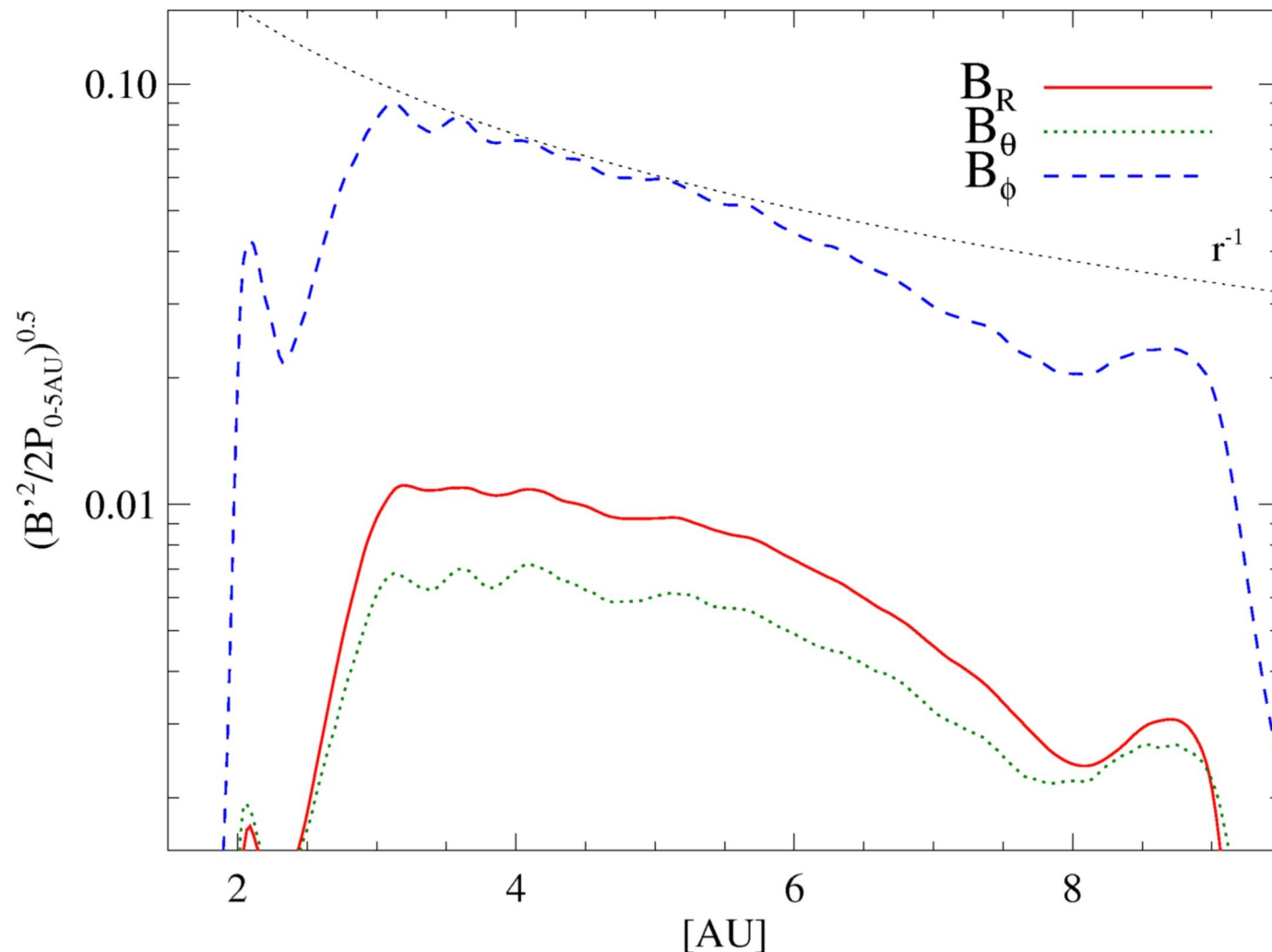
$$\alpha = \frac{\int \rho \left(\frac{v'_\phi v'_R}{c_s^2} - \frac{B'_\phi B'_R}{4\pi\rho c_s^2} \right) dV}{\int \rho dV}$$

Reynolds Stress Maxwell Stress

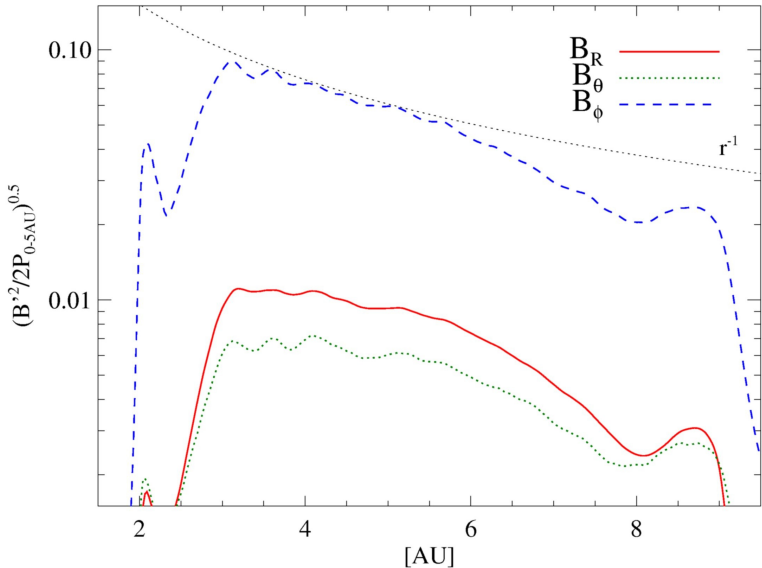


I. α profile

- Vertical profile
- Radial profile



I. α profile

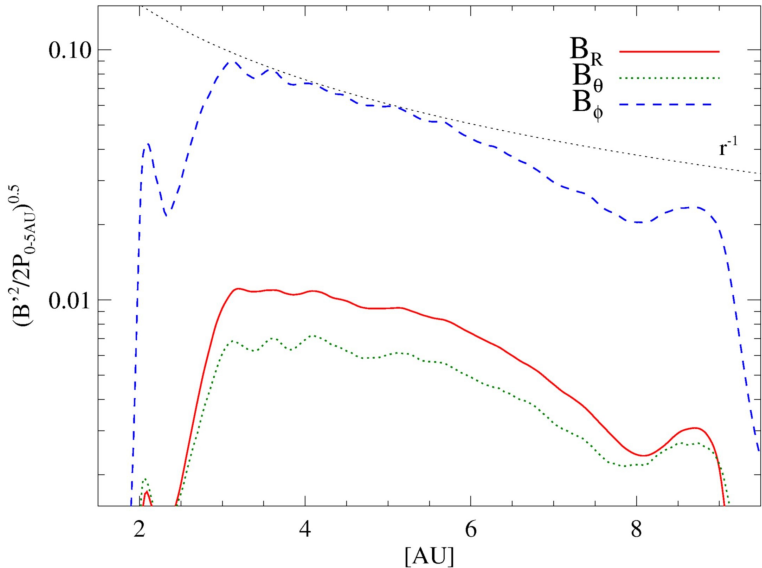


$$F_{\text{radial}} = -\frac{1}{r^2 \rho} \frac{\partial r^2 B_\phi^2}{\partial r}$$



Force-free configuration

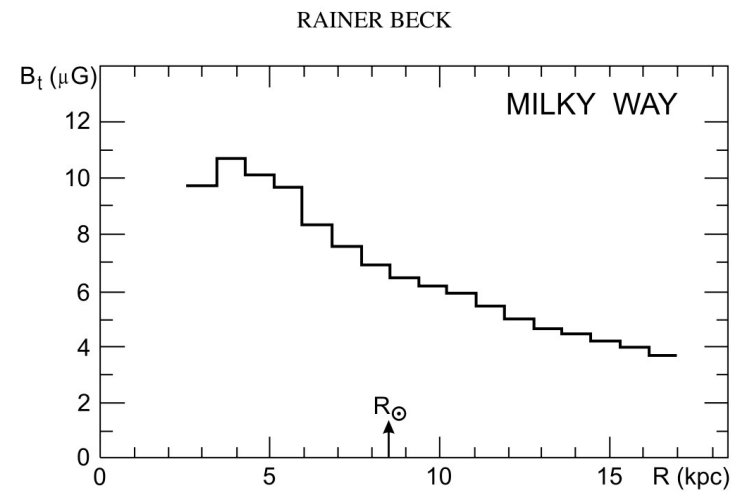
I. α profile



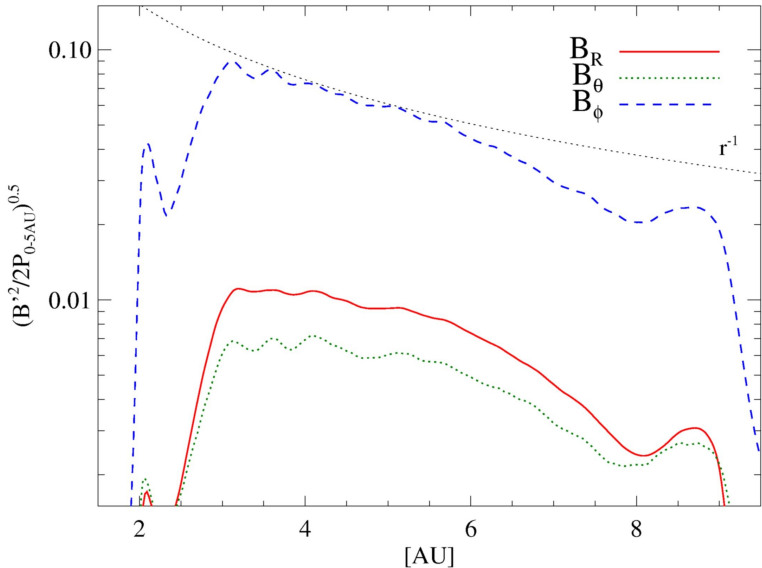
$$F_{\text{radial}} = -\frac{1}{r^2 \rho} \frac{\partial r^2 B_\phi^2}{\partial r}$$



Force-free configuration



I. α profile



$$F_{\text{radial}} = -\frac{1}{r^2 \rho} \frac{\partial r^2 B_\phi^2}{\partial r}$$

→ Force-free configuration

$$\alpha = \frac{\int \rho \left(\frac{v'_\phi v'_R}{c_s^2} - \frac{B'_\phi B'_R}{4\pi \rho c_s^2} \right) dV}{\int \rho dV} \rightarrow \boxed{r^{-2}}$$

I. α profile

Reynolds Stress Maxwell Stress

$$\alpha = \frac{\int \rho \left(\frac{v'_\phi v'_R}{c_s^2} - \frac{B'_\phi B'_R}{4\pi\rho c_s^2} \right) dV}{\int \rho dV}$$

I. α profile

$$\alpha = \frac{\int \rho \left(\frac{v'_\phi v'_R}{c_s^2} - \frac{B'_\phi B'_R}{4\pi\rho c_s^2} \right) dV}{\int \rho dV} \longrightarrow \text{Pressure P}$$

I. α profile

Locally isothermal,
set by initial conditions

$$\alpha = \frac{\int \rho \left(\frac{v'_\phi v'_R}{c_s^2} - \frac{B'_\phi B'_R}{4\pi\rho c_s^2} \right) dV}{\int \rho dV}$$

Pressure P

$\partial \ln P / \partial \ln R \sim -2.5$

I. α profile

$$\alpha = \frac{\int \rho \left(\frac{v'_\phi v'_R}{c_s^2} - \boxed{\frac{B'_\phi B'_R}{4\pi\rho c_s^2}} \right) dV}{\int \rho dV}$$

$$\alpha \sim r^{-2 - \partial \ln P / \partial \ln R}$$

I. α profile

$$\alpha = \frac{\int \rho \left(\frac{v'_\phi v'_R}{c_s^2} - \boxed{\frac{B'_\phi B'_R}{4\pi\rho c_s^2}} \right) dV}{\int \rho dV}$$

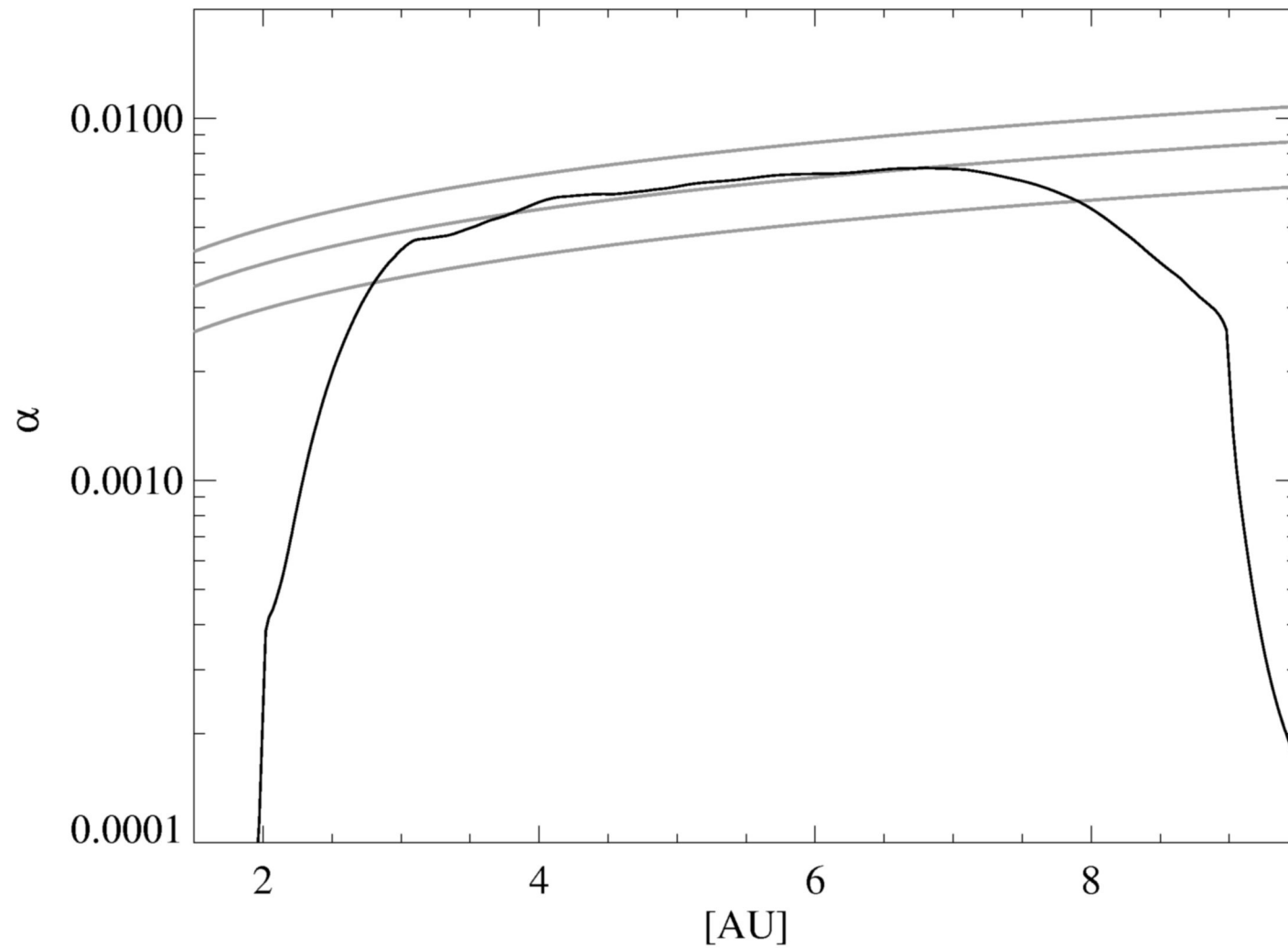


$$\alpha \sim r^{-2 - \partial \ln P / \partial \ln R}$$

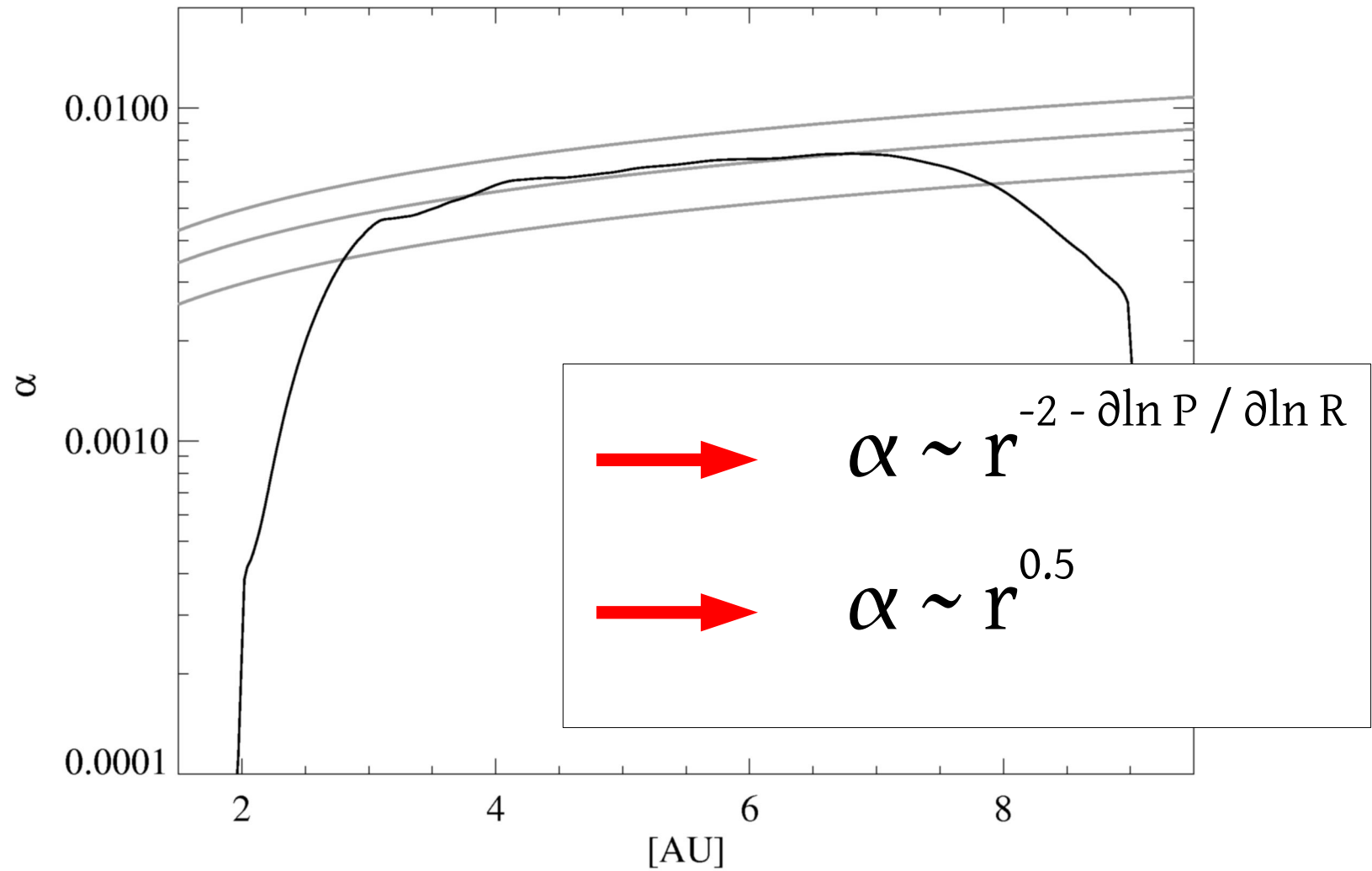


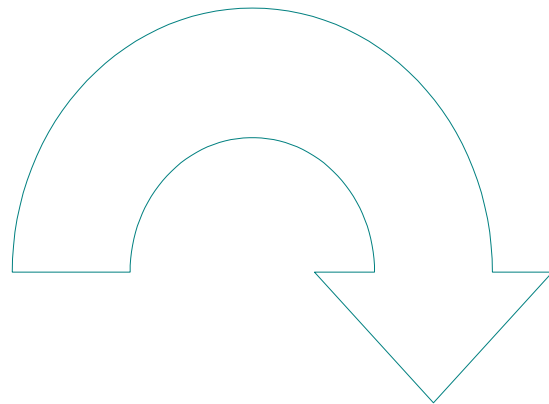
$$\alpha \sim r^{0.5}$$

I. α profile

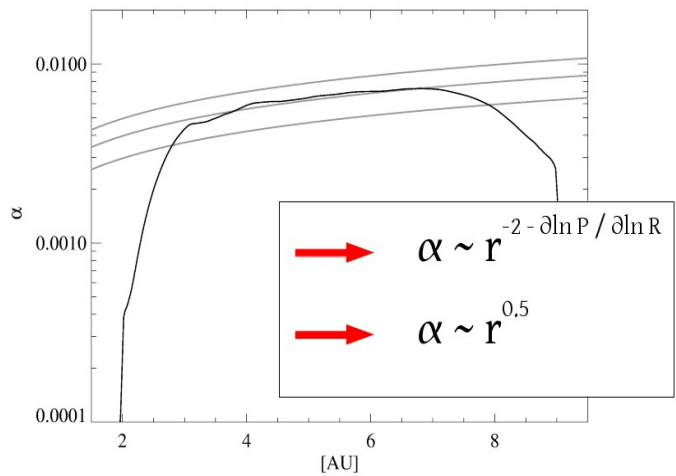


I. α profile





I. α profile



II. Accretion Flows

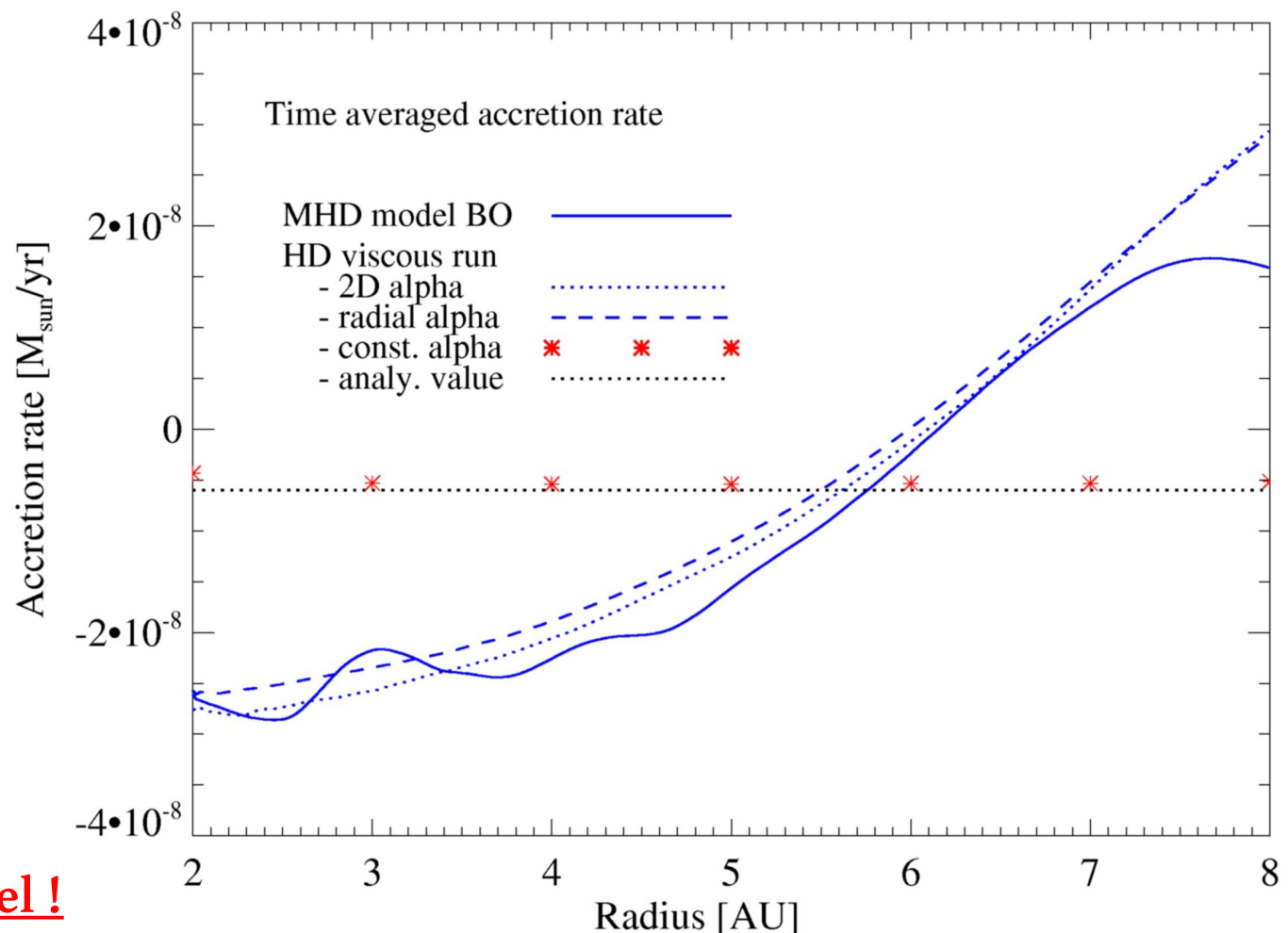
- Total radial accretion
- Radial accretion over height

II. Accretion Flows

- Total radial accretion
- Radial accretion over height

II. Accretion Flows

- Total radial accretion
- Radial accretion over height



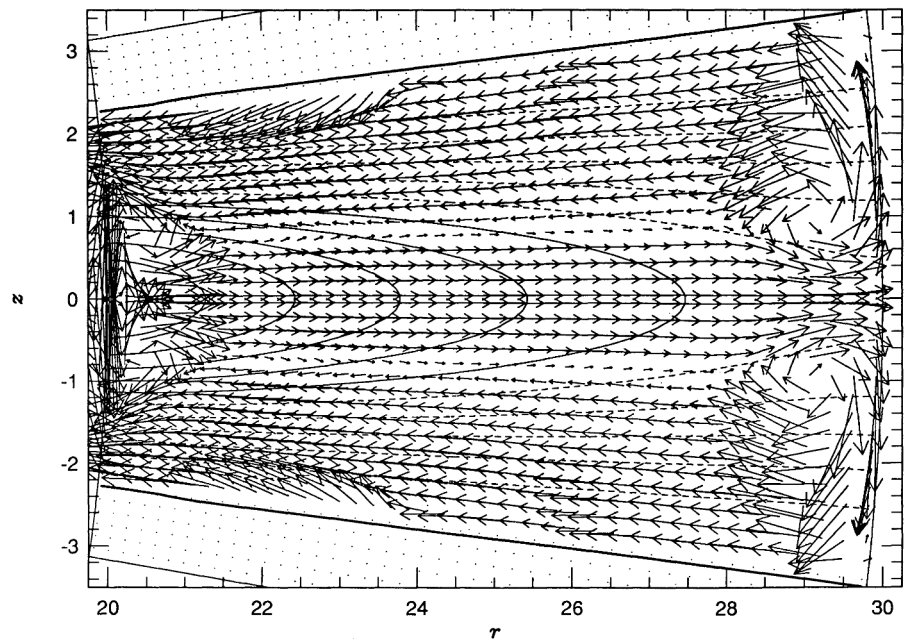
Radial viscosity profile
(HD viscous simulations)
reproduce radial
accretion rate of MHD model !

II. Accretion Flows

- Total radial accretion
- Radial accretion over height

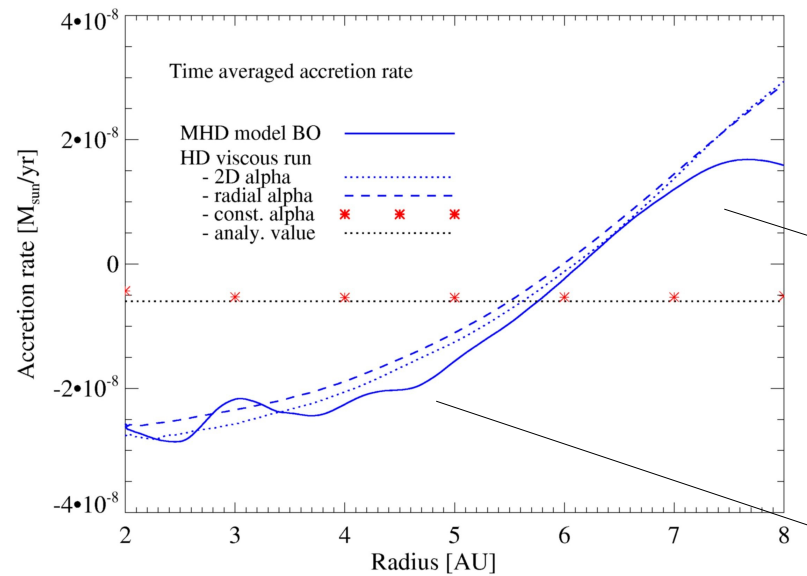
Picture from viscous disk models

- constant accretion rate
- **meridional flows (2D viscous HD simulations)**
- Kley & Lin 1992
- transport of solids (Keller & Gail 2004 , Ciesla 2009)

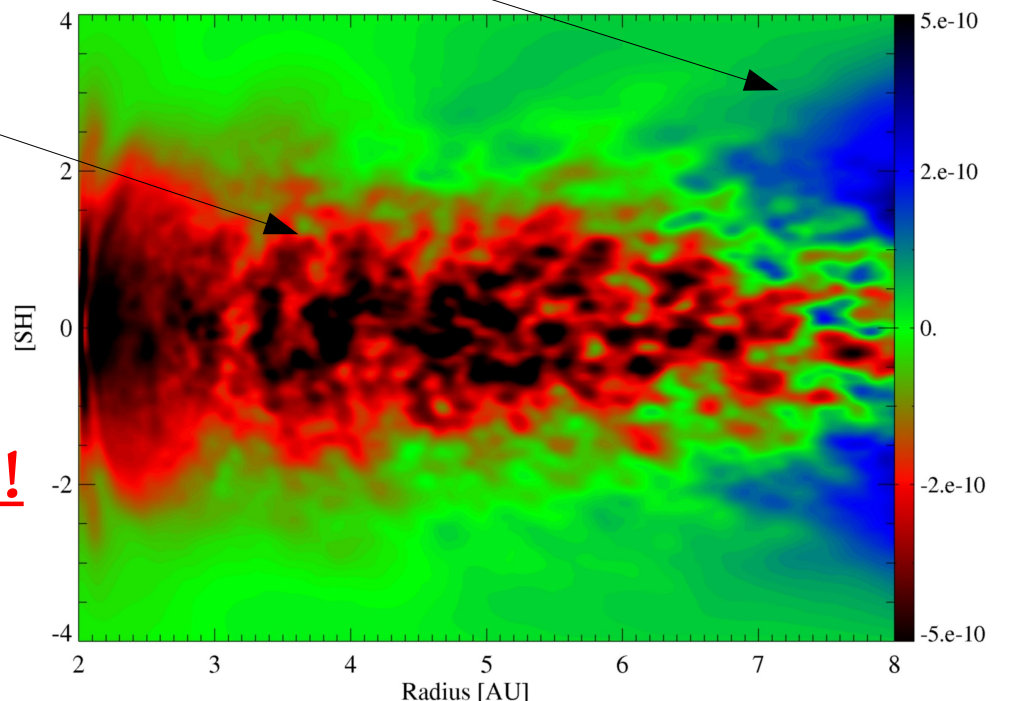


II. Accretion Flows

- Total radial accretion
- Radial accretion over height

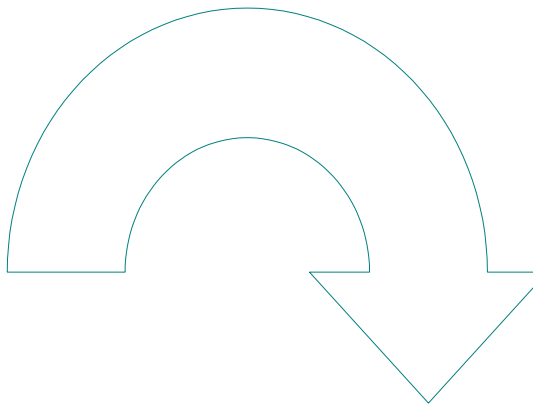


Red – inward motion
Blue – outward motion



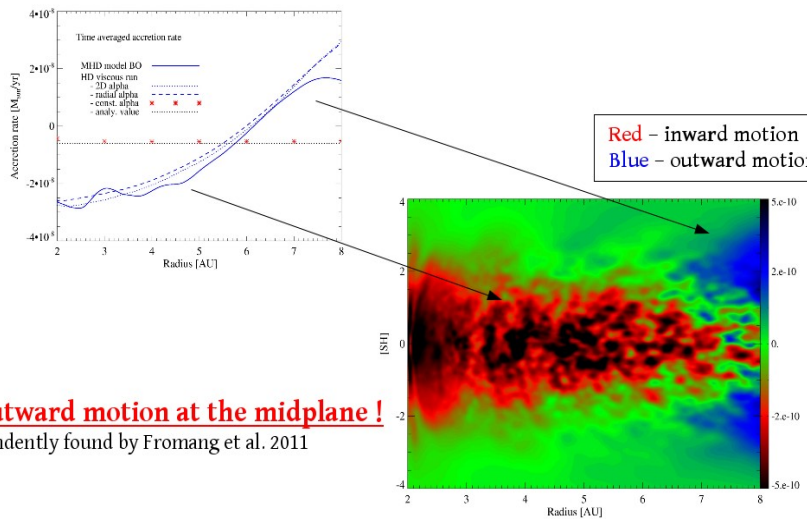
No outward motion at the midplane !

Independently found by Fromang et al. 2011



II. Accretion Flows

- Total radial accretion
- Radial accretion over height

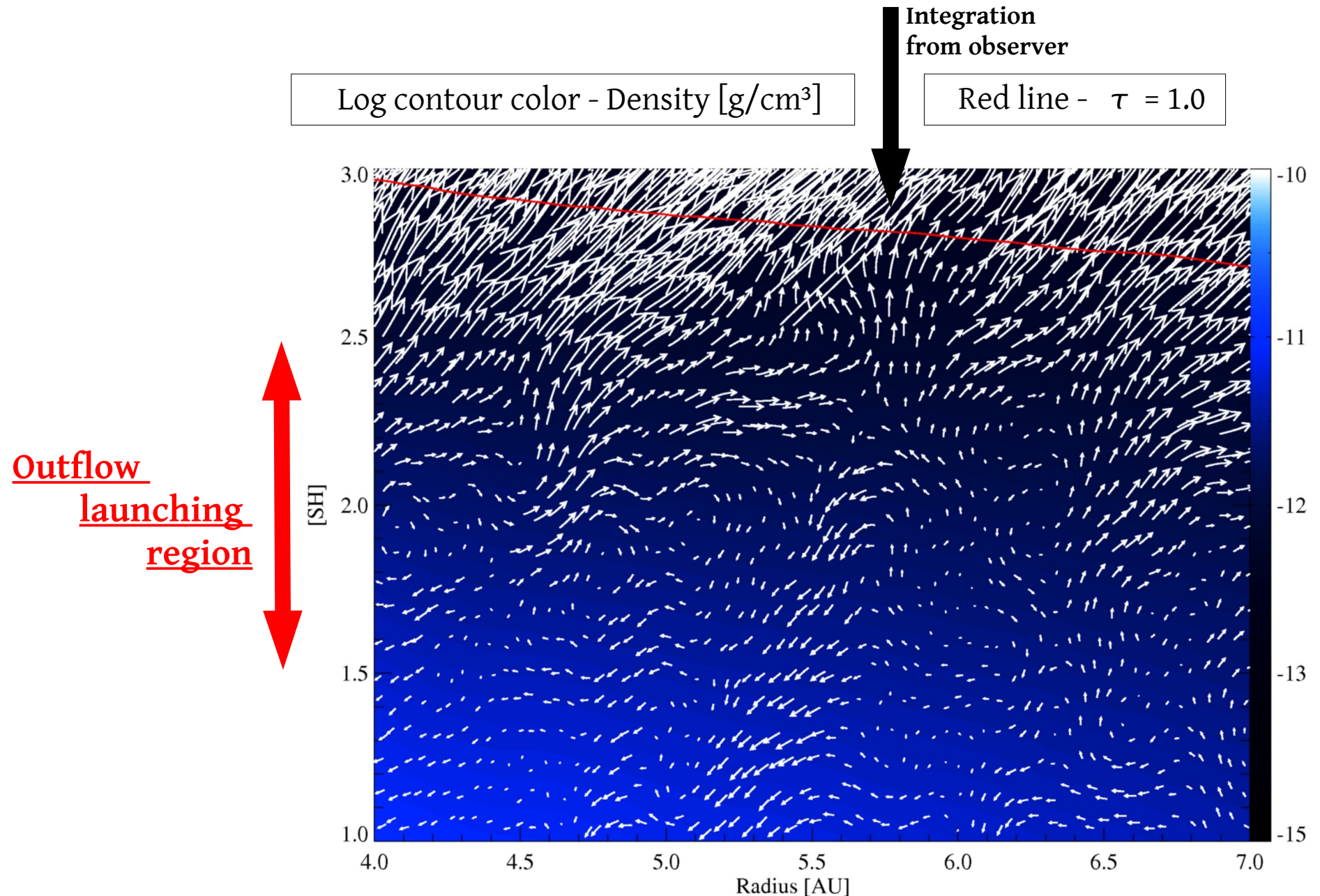


No outward motion at the midplane !

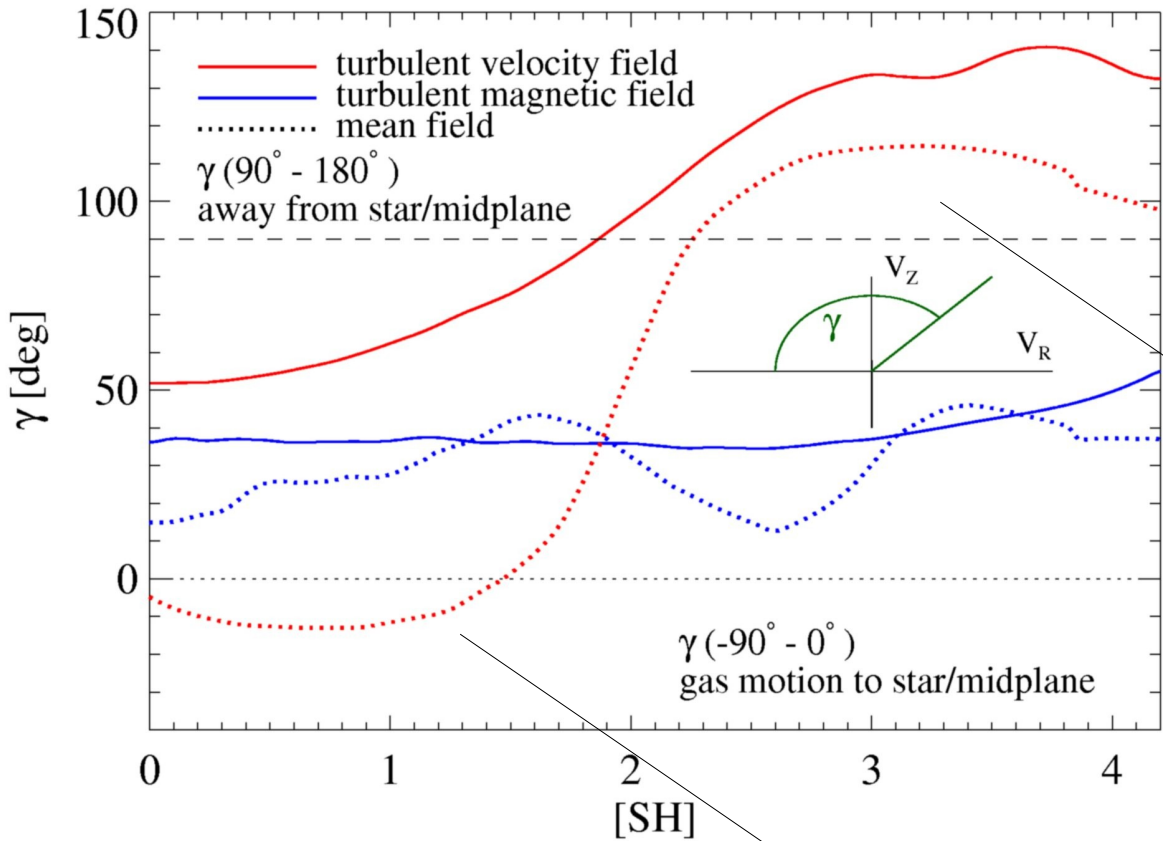
Independently found by Fromang et al. 2011

III. Outflows

III. Outflows



III. Outflows



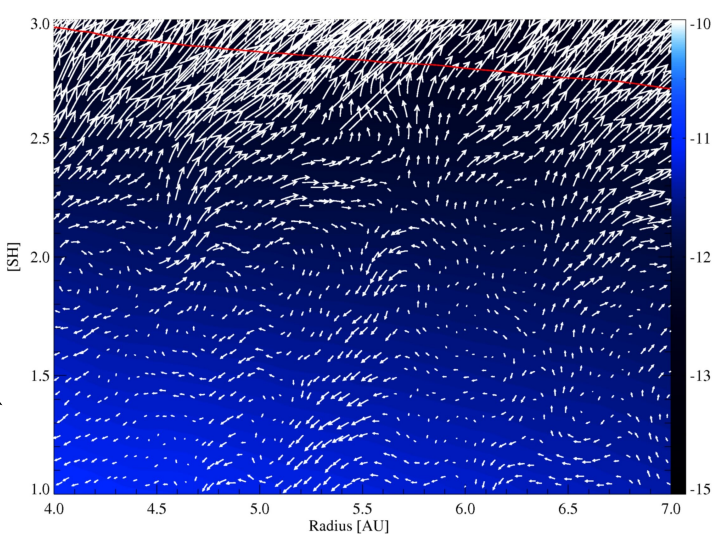
Disk Wind ?

→ Escape velocity not reached

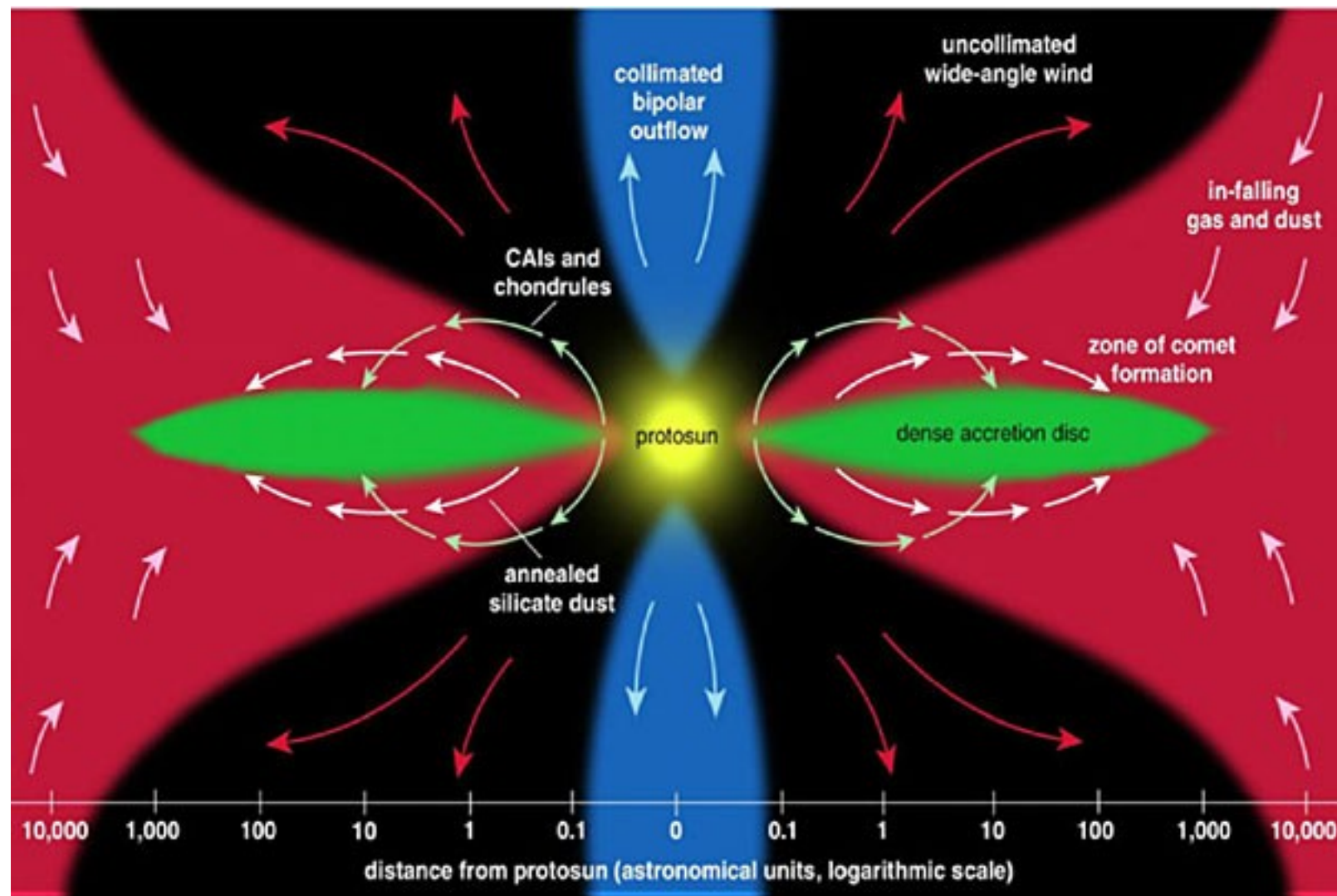
→ **Evaporation time ~2000 local orbits**

→ Suzuki & Inutsuka (2009,2010)

→ Disk wind in local box MRI simulations

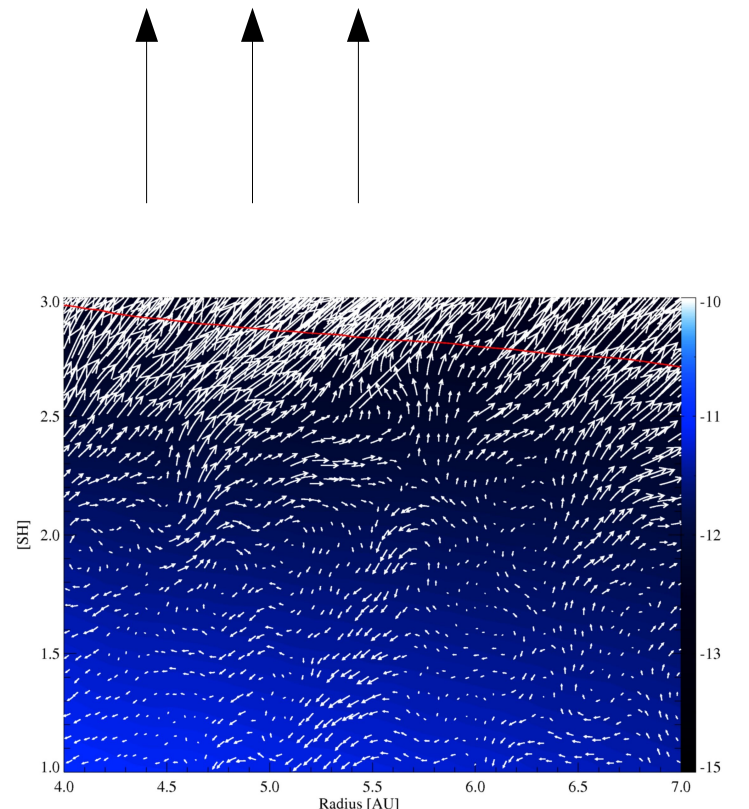
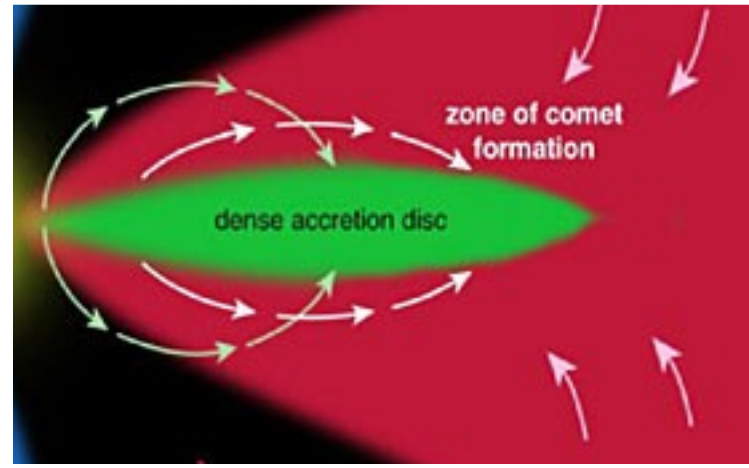
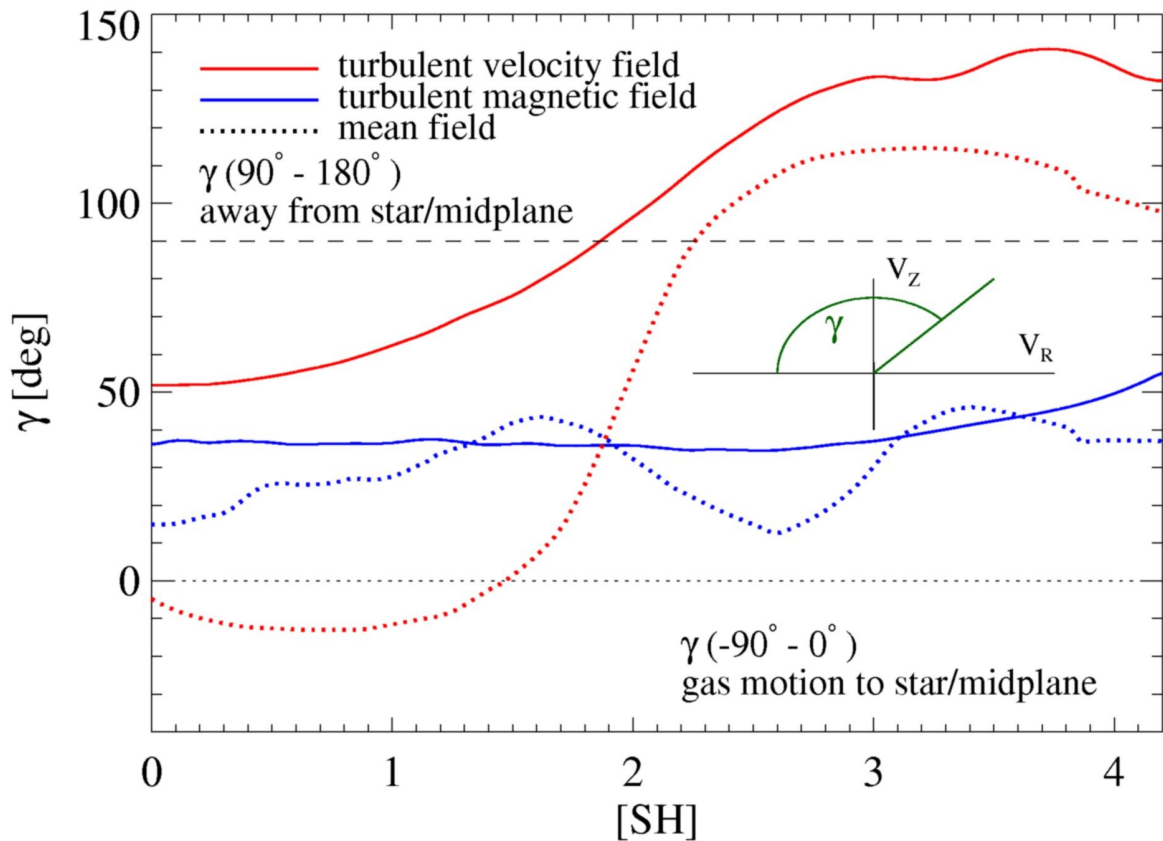


III. Outflows



(from Nuth, J. A., 2001, *American Scientist*, v. 89, p.230.)

III. Outflows



Disk Wind ?

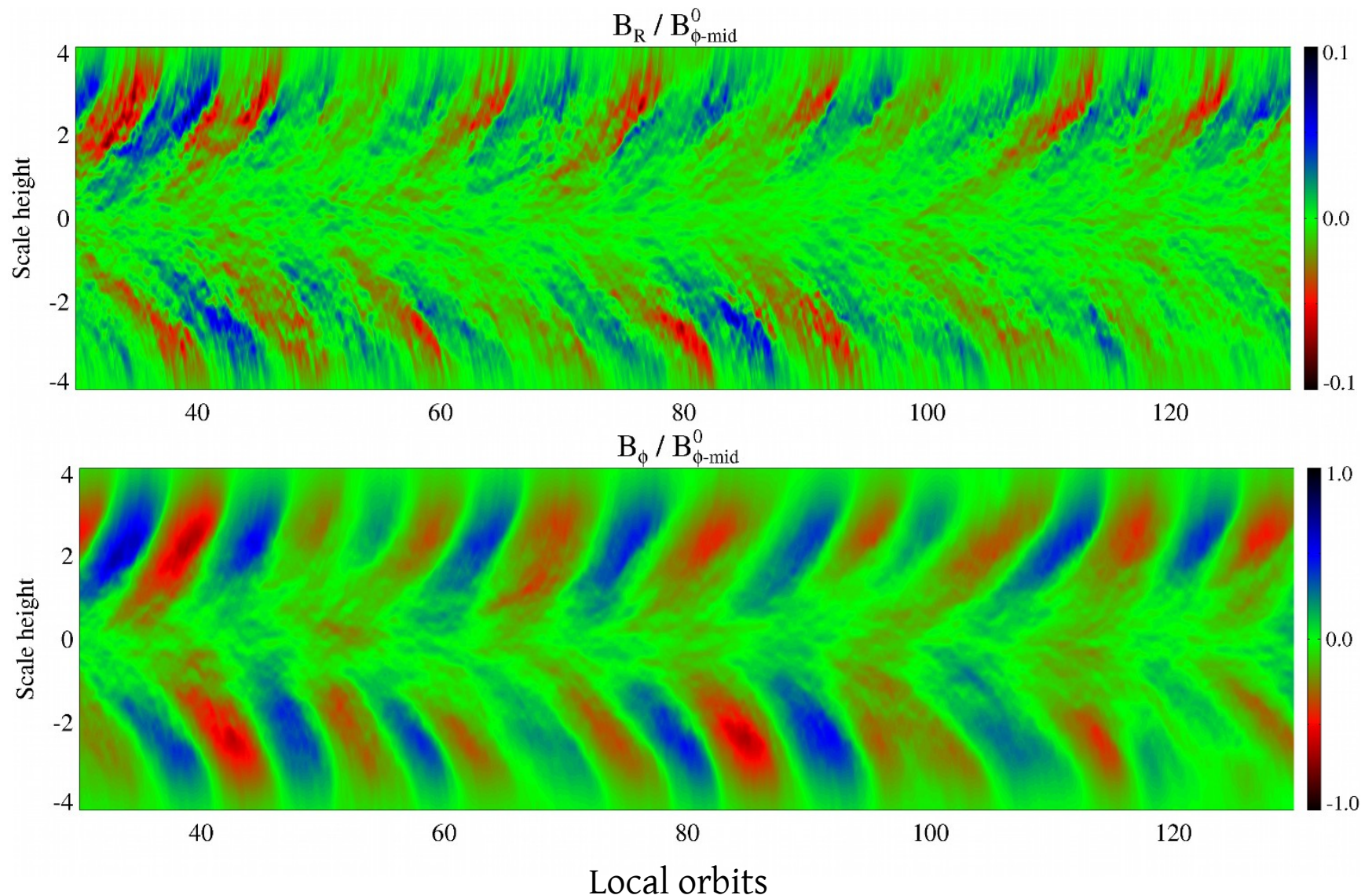
- Escape velocity not reached
- **Evaporation time ~2000 local orbits**
- Suzuki & Inutsuka (2009,2010)
- Disk wind in local box MRI simulations

IV. Dynamo

- Mean field evolution
- Dynamo coefficients
- MRI amplification

IV. Dynamo

- Mean field evolution



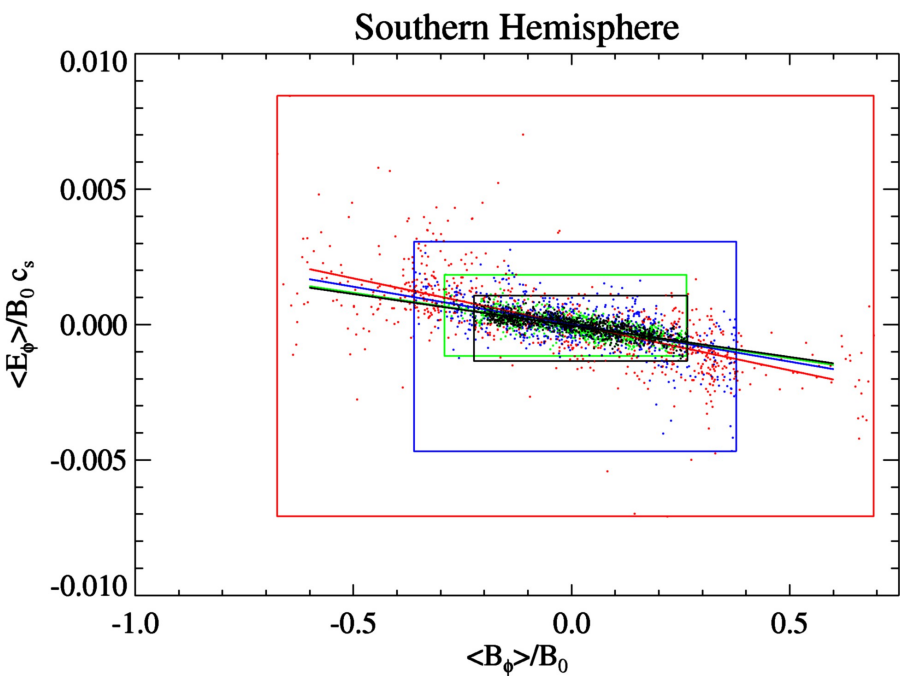
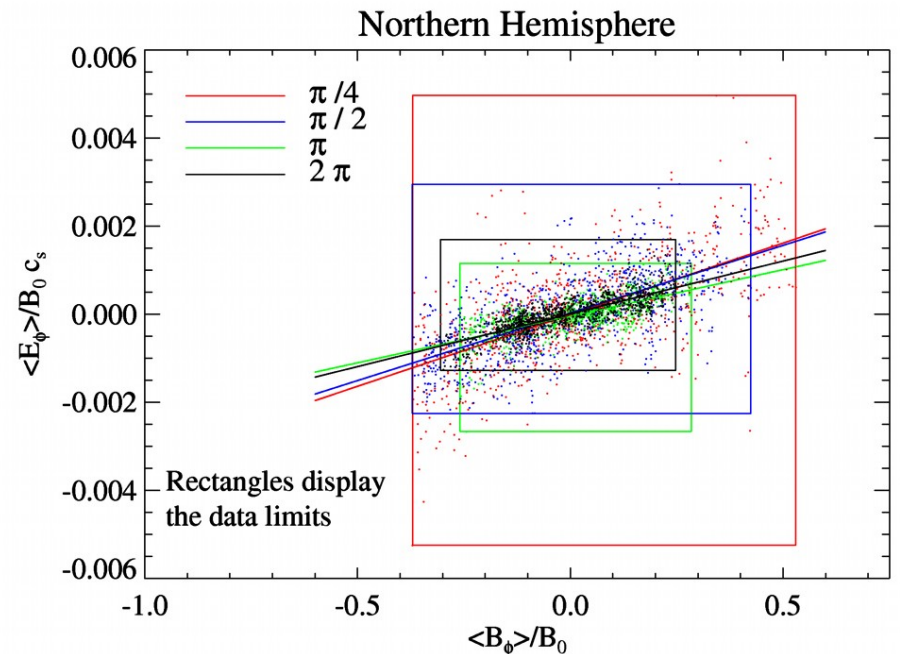
IV. Dynamo

- Dynamo coefficients

Positive in the northern hemisphere

$$\overline{E'_\phi} = \alpha_{\phi\phi}^{\text{dyn}} \overline{B_\phi} + \text{higher derivatives}$$

$$E'_\phi = v'_r B'_\theta - v'_\theta B'_r$$

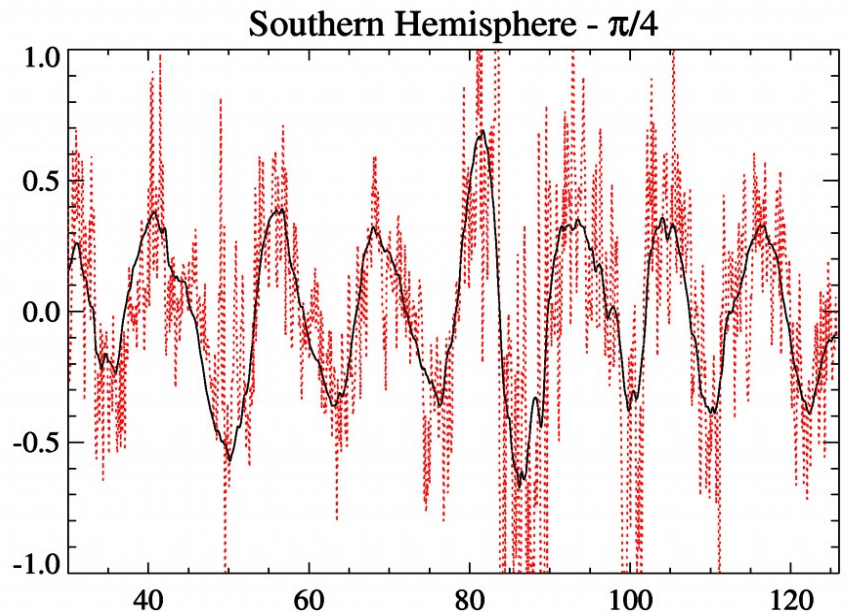
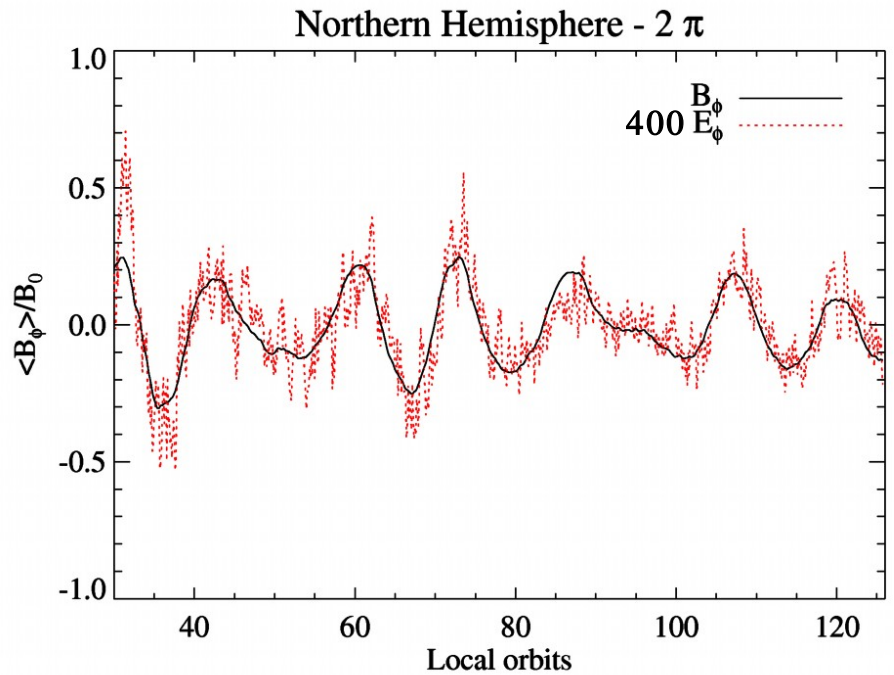


IV. Dynamo

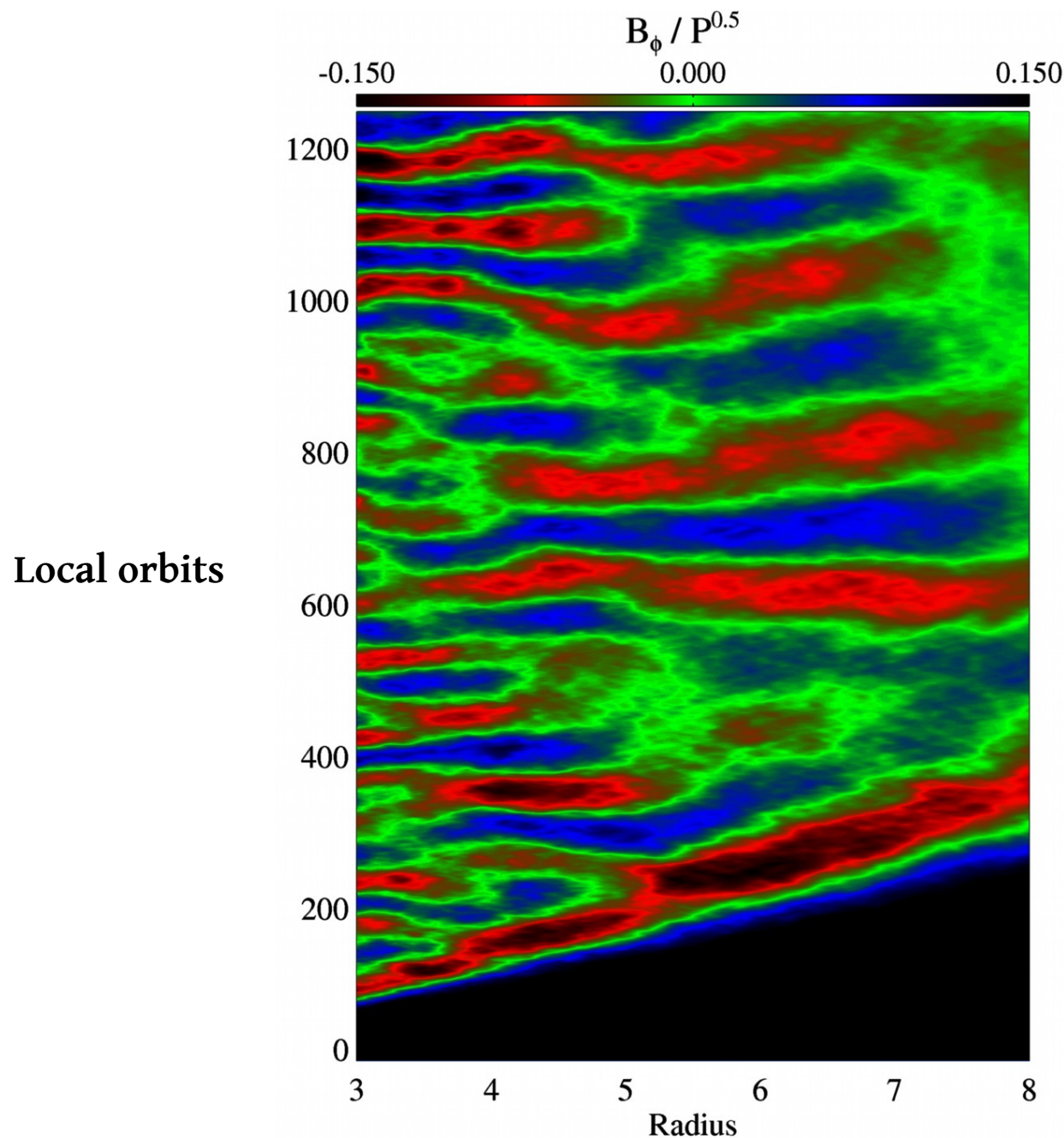
- Dynamo coefficients

$$\overline{E'_\phi} = \alpha_{\phi\phi}^{\text{dyn}} \overline{B_\phi} + \text{higher derivatives}$$

$$E'_\phi = v'_r B'_\theta - v'_\theta B'_r$$

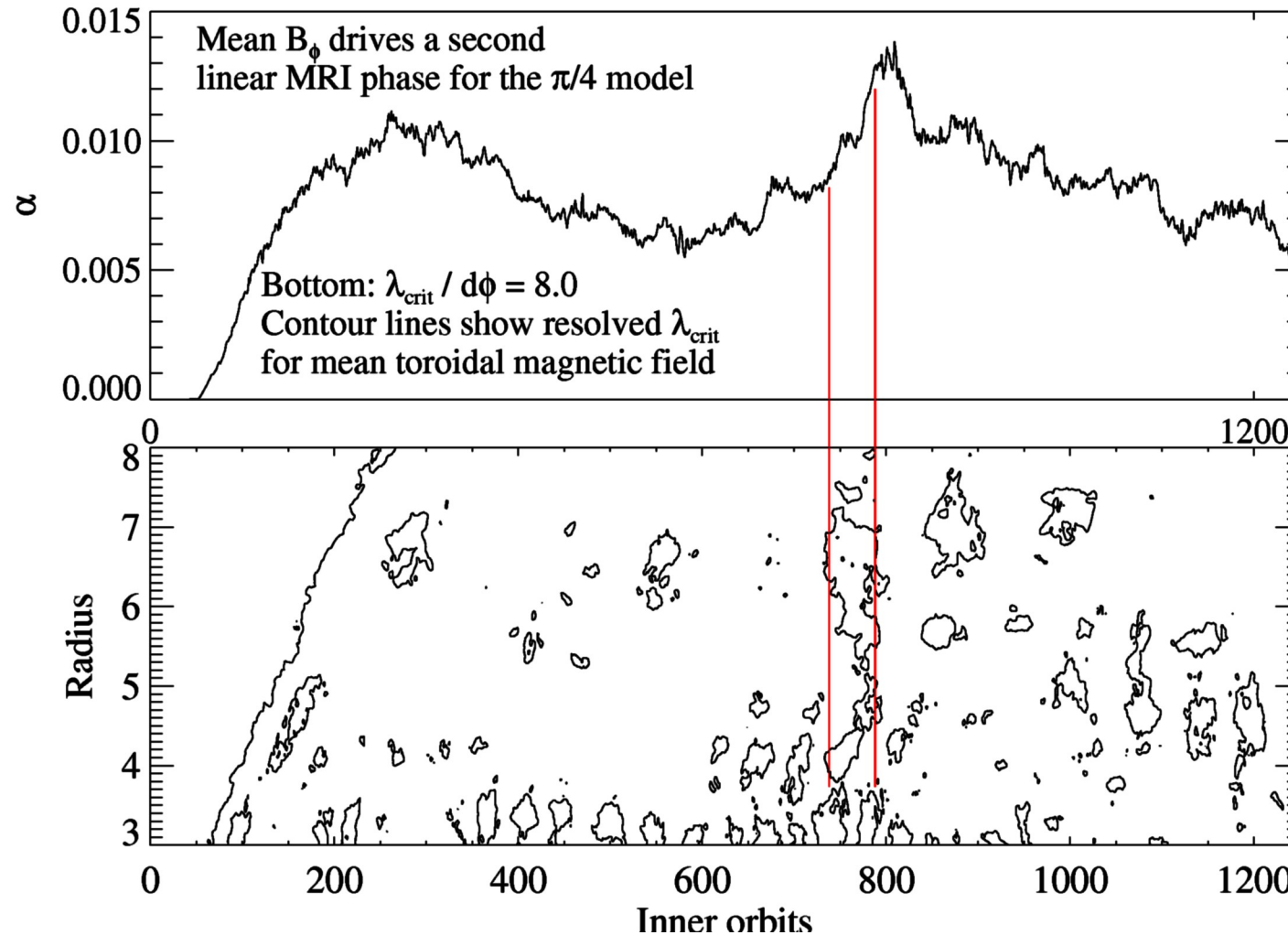


IV. Dynamo

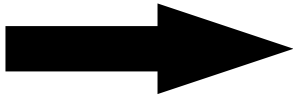


IV. Dynamo

- MRI amplification



Summary

1. We observe a MRI driven outflow.
Possible disk wind ?
2. We see no outflow at the midplane in
3D stratified MHD simulations.
3. In ionized MRI turbulent disk regions we expect $B \sim 1/R$
 $\alpha \sim r^{-2 - \partial \ln P / \partial \ln R}$
4. Dynamo can temporal increase the mass accretion rate.
Amplitude resolution dependent ?

Thanks for your attention ☺

Some words to dynamo coefficients and dynamo number.

In 2π model, we measure:

$$\alpha_{\phi\phi} = 2.3 \times 10^{-3} \text{ [AU/yr]}$$

and

$$V_{\text{RMS}} = 0.113c_s$$

$$\tau_{\text{corr}} = 1.5/\Omega$$

Turbulent magnetic diffusivity is (See Elster et al 1996)

$$\eta_0 = 0.3V_{\text{RMS}}^2\tau_{\text{corr}} = 0.0058H^2\Omega$$

Time to evolve a disk within 4.5 AU will take

$$T_{ev} = R^2/\eta_0 = 3719 \text{ years.}$$

Dynamo numbers at 4.5 AU are :

$$C_\alpha = \frac{\alpha H}{\eta_0} = 12.13$$

$$C_\Omega = \frac{\Omega H^2}{\eta_0} = 174.03$$

Dynamo number $D = C_\Omega C_\alpha = 2111$.

Elstner et al 1996 finds for $D = 5000$, $C_\Omega = 500$, and $C_\alpha = 10$ oscillatory dipolar solution for galactic dynamo.